Physico-chemistry from initial bacterial adhesion to surface-programmed biofilm growth

Carniello, Vera; Peterson, Brandon W.; van der Mei, Henny C.; Busscher, Henk J.

Published in:
Advances in Colloid and Interface Science

DOI:
10.1016/j.cis.2018.10.005

Publication date:
2018

Advances in Colloid and Interface Science 261 (2018) 1–14

Contents lists available at ScienceDirect

Advances in Colloid and Interface Science

journal homepage: www.elsevier.com/locate/cis

Historical Perspective

Physico-chemistry from initial bacterial adhesion to surface-programmed biofilm growth

Vera Carniello, Brandon W. Peterson, Henny C. van der Mei *, Henk J. Busscher

University of Groningen, University Medical Center Groningen, Department of BioMedical Engineering, Groningen, the Netherlands

ARTICLE INFO

Available online 24 October 2018

Keywords:
Biofilm
Surface-sensing
Physico-chemical interactions
Appendages
Tethers
EPS

ABSTRACT

Biofilm formation is initiated by adhesion of individual bacteria to a surface. However, surface adhesion alone is not sufficient to form the complex community architecture of a biofilm. Surface-sensing creates bacterial awareness of their adhering state on the surface and is essential to initiate the phenotypic and genotypic changes that characterize the transition from initial bacterial adhesion to a biofilm. Physico-chemistry has been frequently applied to explain initial bacterial adhesion phenomena, including bacterial mass transport, role of substratum surface properties in initial adhesion and the transition from reversible to irreversible adhesion. However, also emergent biofilm properties, such as production of extracellular-polymeric-substances (EPS), can be surface-programmed. This review presents a four-step, comprehensive description of the role of physico-chemistry from initial bacterial adhesion to surface-programmed biofilm growth: (1) bacterial mass transport towards a surface, (2) reversible bacterial adhesion and (3) transition to irreversible adhesion and (4) cell wall deformation and associated emergent properties. Bacterial transport mostly occurs from sedimentation or convective-diffusion, while initial bacterial adhesion can be described by surface thermodynamic and Derjaguin—Landau—Verwey—Overbeek (DLVO)-analyses, considering bacteria as smooth, inert colloidal particles. DLVO-analyses however, require precise indication of the bacterial cell surface, which is impossible due to the presence of bacterial surface tethers, creating a multi-scale roughness that impedes proper definition of the interaction distance in DLVO-analyses. Application of surface thermodynamics is also difficult, because initial bacterial adhesion is only an equilibrium phenomenon for a short period of time, when bacteria are attached to a substratum surface through few surface tethers. Physico-chemical bond-strengthening occurs in several minutes leading to irreversible adhesion due to progressive removal of interfacial water, conformational changes in cell surface proteins, re-orientation of bacteria on a surface and the progressive involvement of more tethers in adhesion. After initial bond-strengthening, adhesion forces arising from a substratum surface cause nanoscopic deformation of the bacterial cell wall against the elasticity of the rigid peptidoglycan layer positioned in the cell wall and the intracellular pressure of the cytoplasm. Cell wall deformation not only increases the contact area with a substratum surface, presenting another physico-chemical bond-strengthening mechanism, but is also accompanied by membrane surface tension changes. Membrane-located sensor molecules subsequently react to control emergent phenotypic and genotypic properties in biofilms, most notably adhesion-associated ones like EPS production. Moreover, also bacterial efflux pump systems may be activated or mechano-sensitive channels may be opened upon adhesion-induced cell wall deformation. The physico-chemical properties of the substratum surface thus control the response of initially adhering bacteria and through excretion of autoinducer molecules extend the awareness of their adhering state to other biofilm inhabitants who subsequently respond with similar emergent properties. Herewith, physico-chemistry is not only involved in initial bacterial adhesion to surfaces but also in what we here propose to call "surface-programmed" biofilm growth. This conclusion is pivotal for the development of new strategies to control biofilm formation on substratum surfaces, that have hitherto been largely confined to the initial bacterial adhesion phenomena.

Contents

* Corresponding author at: Department of Biomedical Engineering (FB-40), University Medical Center Groningen, P.O. Box 196, 9700 AD Groningen, the Netherlands.
E-mail address: h.c.van.der.mei@umcg.nl (H.C. van der Mei).

https://doi.org/10.1016/j.cis.2018.10.005

1. Introduction

Bacterial adhesion to surfaces usually forms the onset of major problems, such as microbially-influenced corrosion [1], contamination of drinking water systems [2], oral diseases like caries and gingivitis [3], failure of artificial implants in the human body [4,5] and several other industrial and environmental problems. Alternatively, in other applications like bacterial remediation of soil [6] or in the human microbiome at health [7,8], adhesion of bacteria is highly desirable. Although bacterial adhesion to a substratum surface is generally low, typically in the order of 10^6 bacteria cm^{-2} [9], representing a surface coverage of <1%, initially adhering bacteria can grow out into a mature biofilm with thicknesses up to 300 μm [10,11] and containing 10^{10} bacteria cm^{-2} [12], representing a volumetric density of around 0.3 bacteria μm^{-3}, with emergent properties resulting from the adhering state of bacteria in a biofilm-mode of growth.

Biofilm formation is typically divided into four distinct steps: (1) transport of bacteria towards a substratum surface, (2) reversible bacterial adhesion to a substratum surface, (3) transition from reversible to irreversible bacterial adhesion, (4) cell wall deformation and associated emergent properties which are not predictable from the properties of planktonic bacteria [13], including among others extracellular polymeric substance (EPS; a collective term for extracellular polysaccharides, proteins, lipids and DNA) production, localized gradients of nutrient and oxygen, tolerance and resistance and growth of initial colonizers into a mature biofilm [14] (Fig. 1). For a long time, the involvement of physico-chemistry in biofilm formation has been considered limited to the initial steps, including mass transport and reversible adhesion. Mass transport models have been forwarded assuming bacteria to be similar to inert colloidal particles and validated or invalidated in diverse flow displacement systems [9,15]. Contact angle measurements with liquids on substratum surfaces and bacterial lawns have enabled surface thermodynamic analyses of initial adhesion, also assuming bacteria to be inert colloidal particles [16]. The Derjaguin—Landau—Verwey—Overbeek (DLVO)-theory of colloidal stability has been frequently applied as well, particularly to understand the role of electrostatic double-layer interactions in adhesion [17].

However, bacterial diversity and the complexity of bacterial cell surfaces possessing arrays of surface appendages of different length and composition have impeded the development of a generalized physicochemical model for bacterial adhesion to surfaces. The introduction of

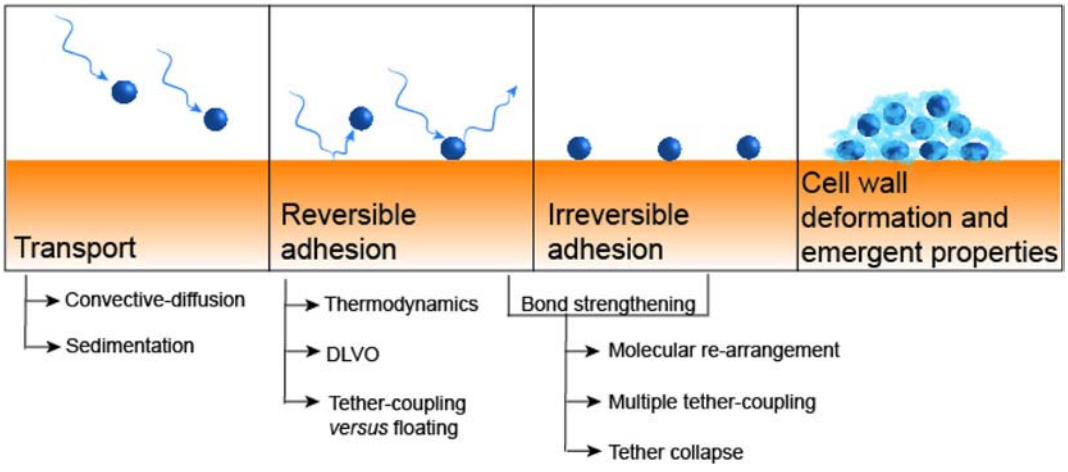

Fig. 1. Four distinct, physico-chemically controlled steps in biofilm formation. (1) Transport of bacteria towards a substratum surface, occurring through convective-diffusion or sedimentation. (2) Reversible bacterial adhesion to a substratum surface, that can be modeled by surface thermodynamics, Lifshitz-Van der Waals and electrostatic double-layer interactions as in the DLVO-theory and tether-coupling or "floating" adhesion models. (3) Transition from reversible to irreversible bacterial adhesion through physico-chemical bond-strengthening mechanisms. (4) After bond-strengthening, cell wall deformation occurs yielding emergent properties, characteristic of a mature biofilm.

the atomic force microscope (AFM) [18] and other instruments, like optical tweezers [19] and the quartz crystal microbalance (QCM) [20], have allowed to analyze the bond properties of bacteria with a substratum surface in terms of adhesion force and viscoelasticity [21,22]. Methods have become available that measure the nanoscopic deformation experienced by bacteria upon their adhesion to surfaces [23], alike the microscopically visible deformation of mammalian cells when they adhere to a surface [24]. Bacterial adhesion force-sensing, associated cell wall deformation and resulting membrane surface tension changes have been suggested to cause adhering bacteria to demonstrate emergent properties that program the properties of a mature biofilm [25], despite the fact that most bacteria in a biofilm are not directly adhering to a substratum surface [26]. Herewith, physico-chemistry can explain many more steps in biofilm formation than mass transport and initial adhesion, extending to emergent biofilm properties, as programmed by the physico-chemistry of the surface to which bacteria adhere.

The aim of this review is to summarize the physico-chemistry involved in the different steps of biofilm formation and integrate the more traditional physico-chemical approaches with new models to yield a comprehensive model of biofilm formation that encompasses mass transport, reversible adhesion, the transition to irreversible adhesion and emergent properties resulting in the formation of a mature biofilm, as programmed by the physico-chemistry of the substratum surface to which biofilm-inhabitants adhere.

2. Bacterial mass transport towards a surface

Biofilm formation begins with bacterial mass transport. In general, bacteria can be transported to a substratum surface as aerosols [27,28], or by sedimentation or convective-diffusion when in an aqueous suspension [9,29]. However, in most applications and experimental studies, bacterial mass transport towards substratum surfaces is studied in aqueous suspensions, and accordingly this review will be confined to bacterial mass transport by sedimentation or convective-diffusion from an aqueous suspension.

Under stagnant conditions, bacterial mass transport from an aqueous suspension is mostly due to sedimentation. In flow displacement systems and under laminar conditions, bacterial mass transport is due to a combination of sedimentation, convection and diffusion [9,30], while under turbulent flow conditions, convective mass transport prevails [31]. Turbulent conditions can be implied from the Reynolds number R_e given by

$$R_e = \frac{U}{(w+h)v} \tag{1}$$

in which U is the volumetric flow rate, w and h are width and depth of the flow displacement system, respectively, and v is the fluid viscosity [31]. When the Reynolds number is smaller than 2000, fluid flow can be considered laminar and the convective-diffusion equation can be solved to calculate mass transport [31]. The generalized convective-diffusion equation reads

$$\frac{\partial C}{\partial t} + \nabla \cdot \boldsymbol{J} = Q \tag{2}$$

in which C is the bacterial concentration, t is the time, $\boldsymbol{J}$ is the flux vector of bacteria, and Q is a source or sink term [32]. Most solutions of the convective-diffusion equation are complicated to obtain and simplified, approximate solutions have been proposed [32]. In the Smoluchowski–Levich (SL) approximation, the contribution of gravity and interaction forces between depositing bacteria and a substratum surface are neglected and perfect-sink conditions are assumed. For a parallel plate flow chamber, these assumptions yield a theoretical SL-deposition rate of bacteria from a flowing suspension equal to

$$j_o^* = 0.538 \frac{D_\infty C}{r} \left(\frac{h\,Pe}{x}\right)^{1/3} \tag{3}$$

in which D_∞ is the bacterial diffusion coefficient, C is the bacterial concentration, Pe is the Peclet number expressing the ratio between convection and diffusion [33], r is the hydrodynamic radius of the bacterium and x is the distance from the inlet of the flow displacement system [31,32,34]. This implies that, in case of sedimentation or strong electrostatic double-layer attraction between negatively-charged bacteria and positively-charged substratum surfaces, the experimentally observed initial deposition rate may exceed the theoretical SL-deposition rate [35]. For bacterial deposition to negatively-charged substratum surfaces, experimental deposition rates are usually smaller than the SL-deposition rates, provided sedimentation is small [36]. For experiments conducted in a parallel plate flow chamber, it has been suggested to average bacterial deposition rates to the top and bottom plate in order to eliminate the influence of sedimentation [37]. Sedimentation also causes an increasing number of depositing and adhering bacteria on the bottom plate of a parallel plate flow chamber with increasing distance from the inlet of the flow chamber, from which bacterial sedimentation velocities can be calculated [38].

In the SL-approximation [32], increasing fluid flow rates yield higher theoretical SL-deposition rates. However, experimentally higher fluid flow rates invalidate the assumption of the substratum surface acting as a perfect-sink, as not all bacteria that are deposited to the substratum surface can withstand the higher shear stress at the surface which discourages their successful adhesion [39]. In *Escherichia coli* for instance, experimental initial deposition rates to a glass surface at low shear rate ($1.5\ s^{-1}$) exceeded SL-deposition rates, while when the shear rate was increased to above $6\ s^{-1}$ the experimental initial deposition rate equaled the SL-deposition rate [15]. The possession of certain types of bacterial surface appendages like flagella enable bacterial swimming and promote faster mass transport to a surface [30,40], that is not accounted for in the SL-approximation. Other types of bacterial surface appendages such as pili, fimbriae or fibrils occurring in *E. coli*, *Pseudomonas aeruginosa, Pseudomonas putida* or streptococci, are used as a tether to approach a surface more closely. Their small appendage diameter enables them to overcome repulsive electrostatic double-layer interactions, yielding a higher percentage of depositing bacteria to successfully adhere [41–43]. However, also ubiquitously present loops of proteins, polysaccharides of DNA in bacterial EPS as well as patches of lipoteichoic acid may serve as tethers involved in bacterial adhesion to a surface.

Bacterial mass transport decreases as bacterial surface coverage increases and under most experimental conditions, deposition rates after prolonged periods of time reduce to zero, which can either imply absence of further successful deposition leading to adhesion, or a balance between detaching and reversibly adhering bacteria on a substratum surface. Absence of further successful adhesion is due to blocking of available adhesion sites on the substratum surface by already adhering bacteria [44,45], and usually a surface coverage of around 10% [38] is sufficient to cause stationary adhesion numbers. Under static conditions, blocked areas around an adhering bacteria are circular [46], but under flow depositing bacteria can be pushed into higher flow lines above a surface by collisions with adhering bacteria causing a-symmetric blocked areas that are elongated in the direction of flow [46,47], as illustrated in Fig. 2. Accordingly, blocked areas increase with increasing fluid flow velocity [31,48] from 45% of the substratum surface area under static conditions [46] to 99% at high shear rate [15] and with increasing particle size, while decreasing with ionic strength [47] due to reduced electrostatic double-layer

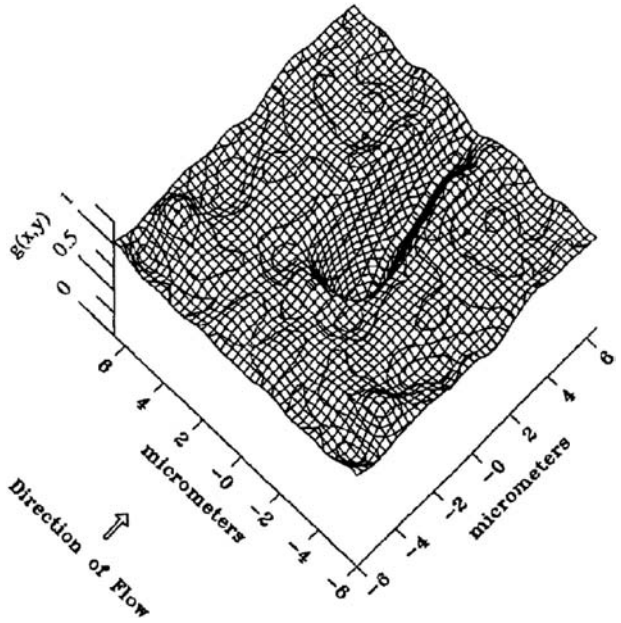

Fig. 2. Blocked areas in bacterial adhesion from a flowing suspension. Blocked area of *S. salivarius* adhering on glass, expressed as a local pair distribution function g(x, y). In a low ionic strength suspension, strong electrostatic double-layer repulsion between flowing and adhering bacteria provoke acceleration of flowing bacteria to flow-lines higher above the surface, yielding an elongation of the blocked area in the direction of flow. The blocked area is evident from the region with g(x, y) smaller than unity around an adhering bacterium located at the origin (0, 0), while g(x, y) = 1 represents the average adhesion number over the entire substratum surface. Adapted from [49] with permission of the publisher, Elsevier.

repulsion between flowing and adhering particles. Alternatively, in case bacteria adhere reversibly, a balance between depositing and successfully adhering bacteria and detaching bacteria may develop, giving rise to a true thermodynamic equilibrium. Importantly, blocking equally occurs in bacterial deposition as well as in the deposition of inert colloidal particles and represents a purely physico-chemical phenomenon [33,46].

3. Reversible bacterial adhesion to a substratum surface

3.1. Surface thermodynamic analysis

Bacterial adhesion is known to be initially reversible. Real-time analysis of bacterial adhesion has shown residence-time dependent desorption [50], while reduction of the bacterial concentration above a substratum surface is known to yield detachment [51], as does increasing fluid shear [52] or the passing of a liquid-air interface over adhering bacteria [53]. Accordingly, in a more traditional physico-chemical approach, initial bacterial adhesion has been regarded as a surface thermodynamic phenomenon for which the required interfacial free energies of adhesion can be acquired from measurement of contact angles with liquids on bacterial lawns, that contain hydrated but condensed bacterial cell surfaces appendages [54]. According to surface thermodynamics (Fig. 3A), conditions are favorable for bacterial adhesion to occur if the interfacial Gibbs free energy of adhesion between bacteria and surface is negative ($\Delta G_{adh} < 0$), while conditions are unfavorable for $\Delta G_{adh} > 0$ [55]. The interfacial Gibbs free energies required can be calculated from contact angle measurements with liquids on the substratum surface and macroscopic lawns of bacteria deposited on membrane filters. Contact angles with different liquids can subsequently be employed in different models, such as the equation of state or the concept of Lifshitz-Van der Waals and acid-base interactions to yield the interfacial free energies from which interfacial Gibbs free energy of adhesion follows [56–59]. Surface thermodynamics requires establishment of an equilibrium situation that includes reversibility of adhesion, but cannot be used to describe the kinetics of adhesion.

3.2. (Extended) DLVO-theory

The DLVO-theory describes bacterial adhesion to surfaces as a results of Lifshitz-Van der Waals, electrostatic-double layer interactions and, in its extended version, acid-base binding [63]. DLVO-analyses are mostly presented as the interfacial Gibbs free energy of adhesion ΔG_{adh} as a function of the separation distance between a bacterium and substratum surface (Fig. 3B), but when taking its first derivative with respect to distance, it represents the interaction force as a function of distance that can be used for analysis of deposition kinetics. Lifshitz-Van der Waals interactions are virtually always attractive [64], while electrostatic double-layer interactions are usually repulsive as nearly all bacterial, synthetic and natural surfaces carry a net, negative surface charge under physiological conditions [65]. However, both bacterial cell surfaces as well as other surfaces can become positively charged depending on pH and ionic strength [66,67]. Acid-base interactions are also often repulsive due to strong electron-donating and relatively small electron-accepting properties of the surfaces involved in bacterial adhesion [68,69]. In the traditional DLVO-theory, the sum total of the Lifshitz-Van der Waals and electrostatic double-layer interactions is a shallow secondary interaction minimum at distances of up to 100 nm [70–72], separated from the substratum surface by an insurmountable primary potential energy barrier. Overcoming the potential energy barrier results in irreversible adhesion, but as long as adhering bacteria reside in the secondary interaction minimum reversibility exists. Bacteria with surface appendages are difficult to capture in the DLVO-theory, as the concept of distance disappears when the cell surface possesses a multi-scale roughness due to surface appendages of different length and widths [73], such as fibrils and fimbriae.

3.3. Tether-coupled versus floating adhesion

Owing to their small diameters [42], single surface appendages have been suggested to be able to "pierce through" the potential energy barrier when an entire bacterium is still in the secondary minimum. Thus surface tethers will reach the deep primary minimum, a few nm adjacent from the substratum surface [42,74] (see Fig. 3B and C). In tether-coupled adhesion, bacteria display harmonic oscillations in the direction perpendicular to the substratum surface [60] from which it can be concluded that surface appendages act as a spring, that also allows restricted motion in the direction parallel to the surface [75]. Tethering of a single cell surface appendage to a substratum surface by piercing through the potential energy barrier, however, likely yields insufficient binding to cause irreversible adhesion and it is usually considered that a single appendage tethered directly to a surface still yields reversible adhesion. Bacteria without surface appendages cannot tether-couple to a substratum surface and will "float" at 1.5 kT (i.e. the thermal energy of a colloidal particle) above a substratum surface, while being captured in the secondary interaction minimum [60]. According to the Boltzmann equation (Eq. 4) [76], their "spontaneous", thermodynamically-driven chances to escape the secondary minimum are proportional with its depth

$$P(z_t - \langle z_t \rangle) = A \ \ exp\left(-\frac{G(z_t - \langle z_t \rangle)}{k_B T}\right) \quad (4)$$

in which A is a normalization constant, $\langle z_t \rangle$ is the equilibrium position of the bacterium perpendicularly to the substratum surface and $G(z_t - \langle z_t \rangle)$ is interfacial Gibbs free energy of adhesion.

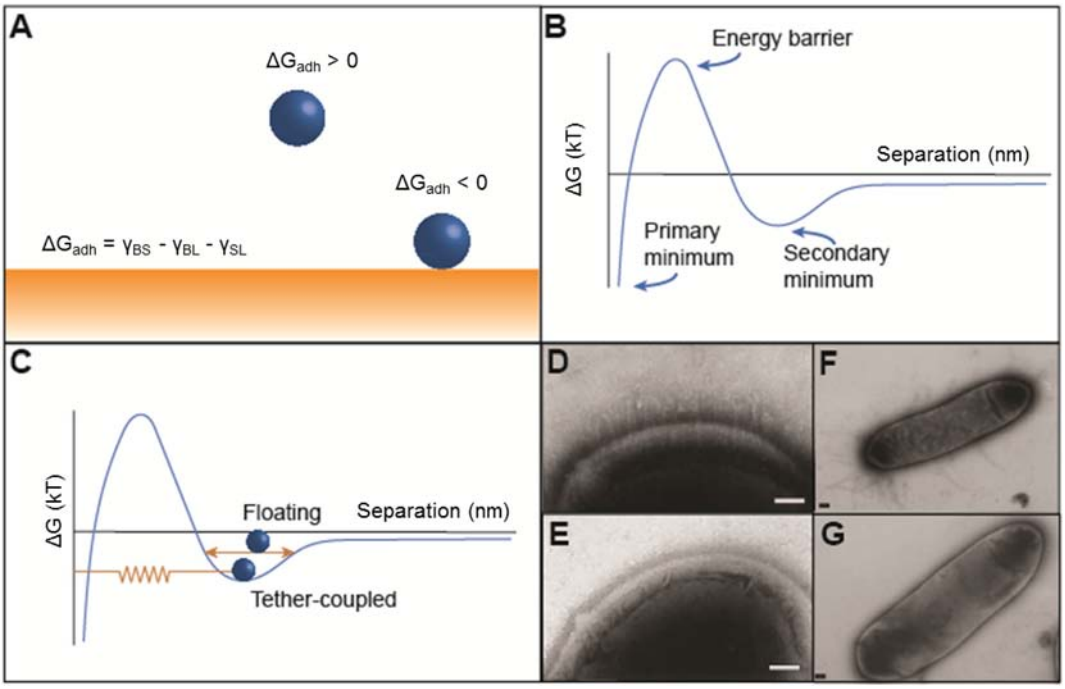

Fig. 3. Physico-chemical models applied to initial bacterial adhesion in its reversible stage. (A) In a surface thermodynamic model, bacterial adhesion is considered favorable when the interfacial energy of adhesion, representing a comparison of the interfacial free energies in the system, is negative. (B) In classical and extended DLVO-theories, bacterial adhesion results from attractive Lifshitz-Van der Waals forces, electrostatic double-layer interactions and acid-base binding. In the classical DLVO-theory, a secondary minimum is discerned in which bacteria are generally assumed to adhere reversibly, with closer approach into the deep, primary interaction minimum being impeded by an insurmountable potential energy barrier. (C) In bacteria possessing cell surface appendages like fibrils or fimbriae (see electron micrographs added for examples in panels D-G), tether-coupling of surface appendages by piercing the potential energy barrier may occur. In tether-coupled bacterial adhesion, the elasticity of the tether forces the distance of the bacterium above the surface to vary according to a harmonic oscillator model, while in floating adhesion, adhering bacteria are confined in their distance variation above a substratum surface by the width of the secondary minimum at 1.5 kT (the thermal energy of a colloidal particle) above its absolute minimum [60]. (D) A *S. salivarius* strain with fibrillar surface appendages. Scale bar indicates 100 nm. Adapted from [61]. (E) A bald *S. salivarius* strain, lacking demonstrable surface appendages. Scale bar indicates 100 nm. Adapted from [61]. (F) A fimbriated E. coli strain. Scale bar indicates 200 nm. Adapted from [62]. (G) A bald E. coli strain, lacking demonstrable surface appendages. Scale bar indicates 200 nm. Adapted from [62]. Electron micrographs reproduced with permission of the publishers, Springer Nature [61] and John Wiley and Sons [62].

4. Transition from reversible to irreversible bacterial adhesion

Both tether-coupled and floating adhesion allow bacteria to transit from a reversible to a more irreversible state of adhesion, as purely based on a variety of different physico-chemical mechanisms that do not yet involve programming of gene expression associated with new emergent properties to enforce binding, such as EPS production [77,78]. The time-scales required for the physico-chemical transition from reversible to more irreversible bacterial adhesion will first be discussed after which different mechanisms underlying the transition will be reviewed.

4.1. Bond-strengtheningtime-scales

Bond-strengtheningtime-scales to more irreversible adhesion have been derived over the past years for a number of different bacterial strains using a variety of entirely different methods that mainly comprise residence-time dependent, thermodynamically-driven desorption or otherwise driven bacterial detachment [34,50,79], residence-time dependent changes in QCM signals upon bacterial adhesion to the crystal surface [80], analysis of retract force-distance curves in bacterial probe AFM taken after different surface-delay times [81–83], calculations of the mean-squared distance traveled by adhering bacteria over a surface as a function of time [41,76] and total internal fluorescence microscopy [84,85] (Fig. 4).

Spontaneous desorption or detachment of adhering bacteria from a substratum surface has been demonstrated to depend on their residence-time on the surface according to [50,86].

$$\beta(t-\tau) = \beta_\infty - (\beta_\infty - \beta_0)\ exp\left(-\frac{(t-\tau)}{\tau_c}\right) \quad (5)$$

in which t is the actual time, τ is the time of arrival of the bacterium on the surface, $(t-\tau)$ is the residence-time, β_0 and β_∞ are initial and final desorption rate coefficients, respectively, and τ_c is the characteristic residence-time (Fig. 4A and B). A residence-time dependence similar to Eq. 5 has also been observed for dissipation signal ΔD when bacteria adhere to a QCM-D crystal surface [80].

$$\Delta D(t-\tau) = \Delta D_\infty - (\Delta D_\infty - \Delta D_0)\ exp\left(-\frac{(t-\tau)}{\tau_c}\right) \quad (6)$$

in which ΔD_0 is the dissipation shift caused by a single bacterium upon arrival on the surface, and ΔD_∞ is the final shift in dissipation. Although the interpretation of the dissipation signal in QCM-D is difficult [20,87,88], it is safe to interpret the signal as indicative of adhering bacteria becoming more closely and more firmly attached to a surface (Fig. 4C and D). Also the confined nanoscopic, Brownian motion of bacteria adhering to substratum surfaces shows a time-dependence, indicating strengthening of their bond,

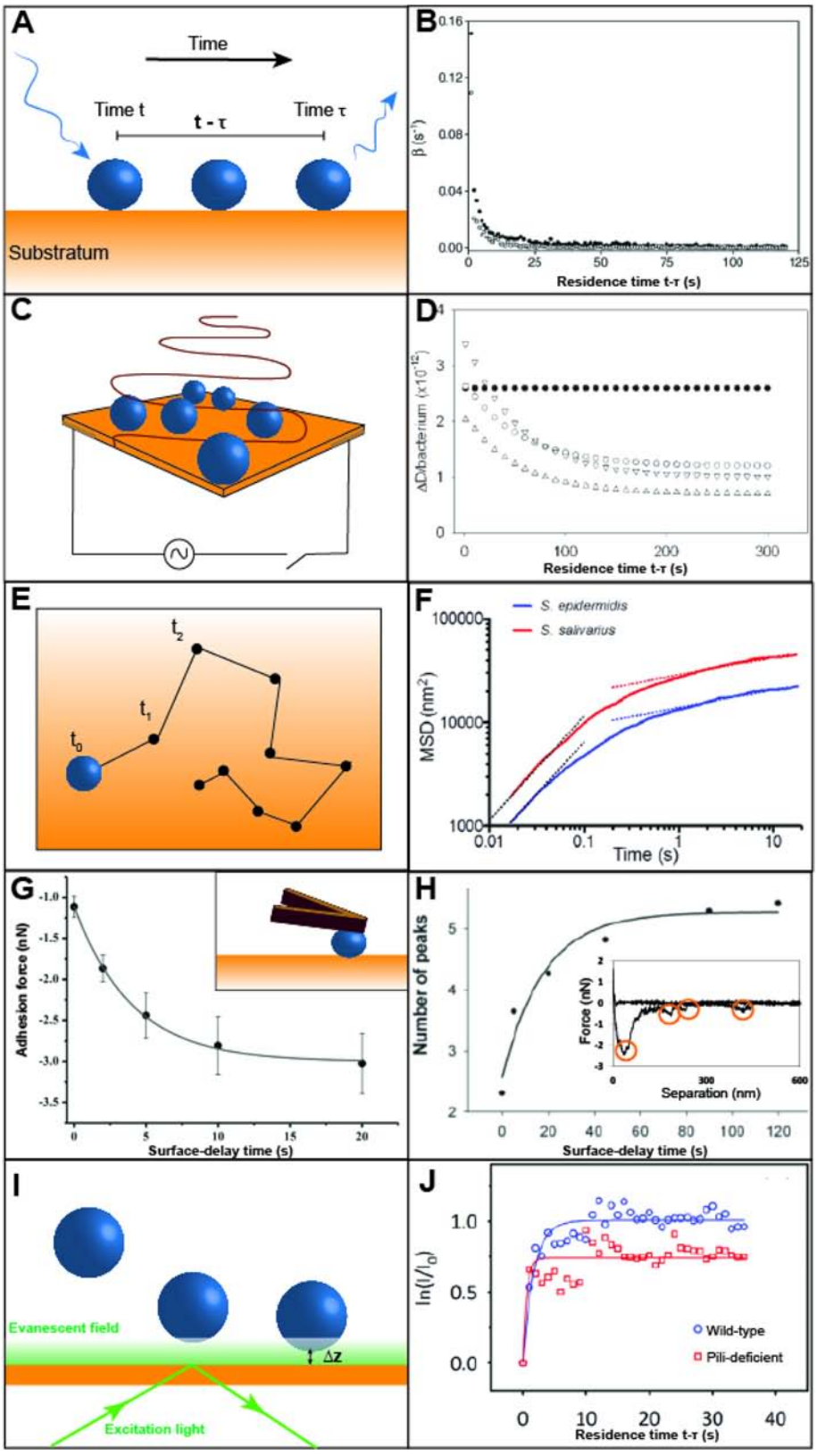
A
Time
Time t
t - τ
Time τ
Substratum
B
β (s⁻¹)
Residence time t-τ (s)
C
D
ΔDbacterium (x10⁻¹²)
Residence time t-τ (s)
E
t0
t1
t2
F
S. epidermidis
S. salivarius
MSD (nm²)
Time (s)
G
Adhesion force (nN)
Surface-delay time (s)
H
Number of peaks
Force (nN)
Separation (nm)
Surface-delay time (s)
I
Evanescent field
Δz
Excitation light
J
ln(I/I0)
Wild-type
Pili-deficient
Residence time t-τ (s)

according to

$$MSD(t) = A \times t^{\alpha} \quad (7)$$

in which $MSD(t)$ is the mean-squared displacement of bacteria as a function of time t, A is a proportionality constant, and α indicates whether the displacement is purely due to diffusion ($\alpha = 1$) or confined by tether-binding ($0 < \alpha < 1$) or absence of displacement ($\alpha = 0$) [41] (Fig. 4E and F). The forces responsible for adhesion and bond-maturation can be directly measured using AFM, while varying the surface-delay time, i.e. the time allowed for the adhesion forces to strengthen themselves. Usually, adhesion forces $F(t)$ increase exponentially with time to a plateau level according to [89].

$$F(t) = F_0 + (F_\infty - F_0)\ exp\left(-\frac{t}{\tau_k}\right) \quad (8)$$

in which F_0 and F_∞ are the adhesion forces before and after bond maturation, respectively, and τ_k is the characteristic time constant (Fig. 4G). Note that adhesion forces as measured by AFM may be 10 to 1000-fold stronger than naturally occurring ones, because the bacterium is wrenched between the surface and the AFM cantilever before retraction of the cantilever [37]. Depending on the strain, substratum and ionic strength in which AFM is carried out, retract force-distance curves demonstrate an increasing number of minor adhesion peaks (Fig. 4H) with surface-delay time [82,90], also considered indicative for a transition towards more irreversible adhesion [91]. Poisson analysis of these minor adhesion peaks in AFM force-distance curves [21,92,93] can be applied to yield the magnitude of acid-base, F_{AB} and long-range, F_{LR} interaction forces when the average adhesion force μ_F is plotted as a function of the variance σ_F^2 over the number of adhesion peaks from different force distance curves taken at one spot according to

$$\sigma_F^2 = \mu_F F_{AB} - F_{AB} F_{LR} \quad (9)$$

Poisson analyses of bacterial adhesion forces measured using AFM have indicated the progressive involvement of acid-base interactions over long-range interactions in the transition from reversible to irreversible adhesion [94].

Example results on bacterial bond-strengthening as listed in Table 1, are also shown in Fig. 4. As can be seen from these examples and the occurrence of exponentially decreasing functions in Eqs. (5), (6) and (8), the transition from reversible to irreversible adhesion will take time, dependent on environmental conditions such as fluid flow. Full loss of reversibility will theoretically require "infinite" time according to Eqs. (5), (6) and (8), and hence the expression "more irreversible" refers to a comparison with the very initial stages of adhesion, and may sometimes be preferable to use than the term "irreversible". Table 1 summarizes the work currently known on time-scales for the physico-chemical transition of reversible towards more irreversible bacterial adhesion, according to different methods and for different bacterial strains, substratum surfaces and in different ionic environments. Importantly, in Table 1, bond-strengthening time-scales have also been presented for inert colloidal particles. Time-scales for inert particles do not differ grossly from those for bacteria, attesting to the physico-chemical nature of the transition towards irreversible bacterial adhesion in this stage of biofilm formation. From Table 1 it can be concluded that the physico-chemical transition from reversible to irreversible adhesion typically occurs on a time-scale of minutes. Surface hydrophobicity, charge and even nanostructuring of the substratum surfaces have only minor impact on the time-scales of bond-strengthening, and similar results are obtained on abiotic and biotic surfaces as well as for adhesion of bacteria to each other ((co-)aggregation).

4.2. Bond-strengthening mechanisms

Bond-strengthening as occurring over the first minutes after adhesion of bacteria to a substratum surface, is a physico-chemical process and there are a number of underlying mechanisms suggested in the literature that contribute to it, that we will now summarize.

4.2.1. Molecular mechanisms

Due to the small molecular size and low viscosity of water, the progressive removal of interfacial water likely takes place within seconds from the first contact of a bacterium with a substratum surface [113]. Removal of interfacial water enables closer approach and the formation of attractive acid-base interactions [80], and may occur more readily on hydrophobic substratum surfaces than on hydrophilic ones [43,81]. Removal of interfacial water to allow bacteria to adhere, may also be one of the reason why many bacteria have been equipped with hydrophobic surface structures to act as a broom removing water, despite being hydrophilic as a whole [114].

Adhesion forces between bovine-serum-albumin-coated microspheres and a substratum surface measured by AFM increased more than of non-coated microspheres [83], demonstrating that not only interfacial water removal but also conformational changes of proteins adjusting themselves to a new surrounding [115] may contribute to bond-strengthening [116,117]. Similarly, eDNA can re-arrange to a more elongated conformation to expose more binding sites towards a substratum surface [102], while finally an entire bacterium may rotate to expose its most adhesive sites to a surface, as occurs for "tufted" bacteria only carrying fibrils on one pole of the cell [118] or bacteria having a heterogeneous surface charge distribution [119]. Collectively, these molecular mechanisms (Fig. 5A) contribute to the progressive coupling of multiple tethers to a surface.

4.2.2. Multiple tether-coupling

Whereas the binding of a single tether does not yield irreversible adhesion of a bacterium to a substratum surface, several types of studies, most notably confined Brownian motion analyses (Fig. 4F) and AFM

Fig. 4. Example results of different methods to determine the time-scales for the physico-chemical transition from reversible bacterial adhesion towards more irreversible adhesion. (A) Schematic presentation of residence-time dependent desorption. (B) Example of the residence-time dependent desorption rate coefficient $\beta(t - \tau)$ for S. epidermidis on hydrophilic glass (black dots) and hydrophobic silanized glass (open dots). Adapted from [50] with permission of the publisher, Elsevier. (C) Schematic presentation of the QCM-D technique. From the oscillation decay over time of an oscillating quartz crystal [87], the intimacy of the bond between bacteria adhering to the crystal surface can be derived as a function of the residence-time of the adhering bacteria on the surface. Adapted from [95]. (D) Residence-time dependent dissipation $\Delta D(t - \tau)$ as measured with QCM-D for densely fibrillated S. salivarius HB7 (○), sparsely fibrillated S. salivarius HBV51 (▽), bald S. salivarius HBC12 (△) and micrometer-sized silica particles (●). Adapted from [80] with permission of the publisher, American Chemical Society. (E) Schematic presentation of confined nanoscopic, Brownian motion of bacteria adhering to substratum surfaces (top view). (F) Mean-squared displacement of bacteria as a function of time for S. epidermidis and S. salivarius. Black dotted lines represent $MSD(t) = A \times t\alpha$ for $\alpha = 1$, while colored dotted lines are fitted to measured MSD values for $t > 5$ s. Adapted from [41] with permission of the publisher, Springer Nature. (G) Example of the adhesion force between E. coli and goethite as a function of surface-delay time. Insert represents a bacterium attached to an AFM cantilever for adhesion force measurement. Adapted from [96] with permission of the publisher, Springer Nature. (H) Development in time of minor adhesion peaks in AFM retraction force-distance curves as a function of bond strengthening. Insert is an example of retraction force-distance curve showing minor adhesion peaks. Adapted from [91] with permission of the publisher, SAGE Publications. (I) Schematic presentation of total internal reflection fluorescence microscopy. An excitation light beam produces an evanescent field at the bacterium-surface interface [97]. The evanescent field intensity decrease exponentially with the distance from the surface, becoming negligible after 150 nm from the surface, enabling accurate determination of the bacterium-surface distance Δz [84]. (J) Total internal reflection fluorescence intensities for wild-type P. aeruginosa and a pili-deficient mutant ΔpilA, as a function of residence time on the surface. Adapted from [84] with permission of the publisher, Elsevier.

Table 1
Overview of time-scales for the physico-chemical transition from reversible bacterial adhesion towards ("more") irreversible adhesion, for different bacterial strains adhering to substratum surfaces with different hydrophobic and charge properties and obtained using different methods.

Substratum properties	Ionic strength (mM)	Time-scale (s)	Strain	References
Residence-time dependent desorption*				
Hydrophilic	10	0.9–1.1	*Staphylococcus epidermidis*	[50]
Hydrophilic	10	5–40	*P. aeruginosa*	[98]
Hydrophilic	40	30	*S. epidermidis*	[34]
Hydrophilic	40	40	*Acinetobacter calcoaceticus*	[34]
Hydrophilic	40	50	Polystyrene particles	[34]
Hydrophilic	40	60	*Streptococcus thermophilus*	[34]
Hydrophilic	40	70	*S. epidermidis*	[34]
Hydrophobic	10	0.7–0.8	*S. epidermidis*	[50]
Hydrophobic	10	5–40	*P. aeruginosa*	[98]
Hydrophobic	40	40	*A. calcoaceticus*	[34]
Hydrophobic	40	40	*S. epidermidis*	[34]
Hydrophobic	40	50	Polystyrene particles	[34]
Hydrophobic	40	60	*S. thermophilus*	[34]
Hydrophobic	Growth medium, not specified	12–13	*Caulobacter crescentus*	[99]
Positively-charged	26	240–300	*Staphylococcus aureus*	[79]
Biopolymer-coated	167	0.9–1.2	*S. aureus*	[100]
Residence-time dependent QCM-d signal analysis				
Hydrophilic	57	50–60	*Streptococcus salivarius*	[80]
Hydrophilic	10–300	100–200	*E. coli*	[101]
Hydrophilic	10–300	100–200	*Sphingomonas wittichii*	[101]
Hydrophilic	Growth medium, not specified	1500–1800	*P. aeruginosa*	[84]
Confined nanoscopic, brownian motion as a function of time				
Hydrophilic	0.57	10	*S. epidermidis*	[41]
Hydrophilic	0.57	10	*S. salivarius*	[41]
Atomic force microscopy-adhesion forces as a function of surface-delay time				
Hydrophilic	1	10	Polystyrene particles	[83]
Hydrophilic	10	5–35	*S. epidermidis*	[89]
Hydrophilic	15	10	*Streptococcus mutans*	[102]
Hydrophilic	100	5	Polystyrene particles	[83]
Hydrophilic	150	90–120	*S. mutans*	[102]
Hydrophilic	167	1	*S. epidermidis*	[81]
Hydrophilic	167	2	*Pseudomonas fluorescens*	[81]
Hydrophilic	167	60–120	*E. coli*	[103]
Hydrophobic	10	5–20	*S. epidermidis*	[89]
Hydrophobic	15	90	*S. mutans*	[102]
Hydrophobic	150	90–120	*S. mutans*	[102]
Hydrophobic	167	10	*Massilia timonae*	[104]
Hydrophobic	167	30–60	*Bacillus subtilis*	[104]
Hydrophobic	167	30–60	*P. aeruginosa*	[104]
Positively-charged	167	60–120	*E. coli*	[103]
Nanopillared	167	10	*S. aureus*	[105]
Nanopillared	167	10	*S. epidermidis*	[105]
Silicon nitride AFM tip	40	100	*S. thermophilus*	[106]
Biopolymer-coated	Low	5–10	*Lactococcus lactis*	[107]
Biopolymer-coated	1	50–100	Polystyrene particles	[108]
Biopolymer-coated	100	5–50	Polystyrene particles	[83,108]
Lactobacilli**	167	30–60	*S. aureus*	[109]
*S. aureus***	167	60–120	*S. aureus*	[109]
*S. mutans***	167	120	*S. mutans*	[110]
Candida albicans hyphae	10	40–60	*P. aeruginosa*	[111]
Endothelial cells	Growth medium, 140 mM (pH 7.4)	600	*S. aureus*	[82]
Atomic force microscopy-development over time of minor adhesion peaks				
Hydrophilic	TRIS-buffer, not specified	60	*Streptococcus sanguinis*	[112]
Saliva-coated enamel	57	90–120	*Streptococcus mitis*	[91]
Saliva-coated enamel	57	90–120	*S. mutans*	[91]
Saliva-coated enamel	57	90–120	*S. sanguinis*	[91]
Saliva-coated enamel	57	90–120	*Streptococcus sobrinus*	[91]
S. mutans	167	120	*S. mutans*	[110]
Total internal reflection fluorescence microscopy				
Hydrophilic	Growth medium, not specified	0.5–2	*P. aeruginosa*	[84]
Hydrophilic	100	0.1–0.2	*E. coli*	[85]

* These experiments have been done using real-time imaging and time-resolution depends on the image-acquisition time.
** These experiments involve adhesion of bacteria to bacteria of the same (aggregation) or of a different strain or species (co-aggregation).

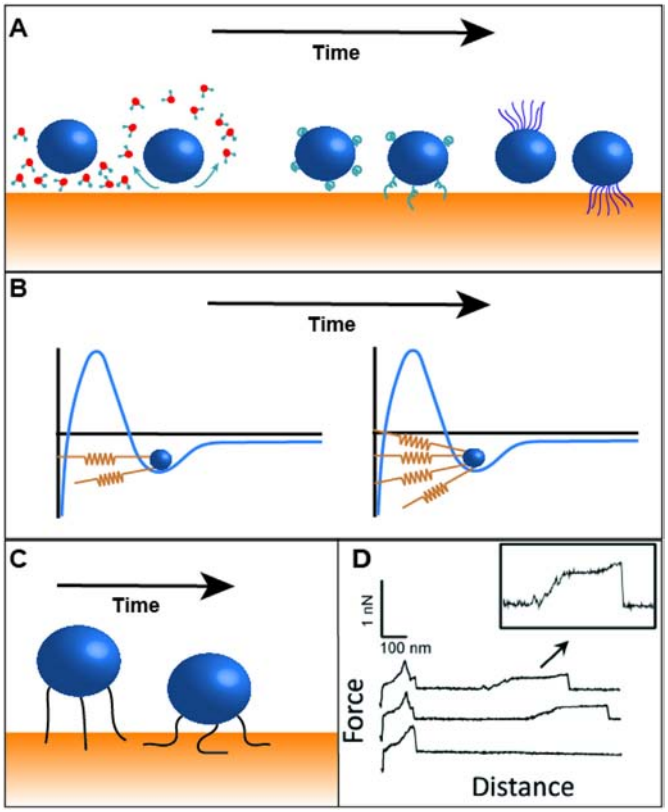

Fig. 5. Physico-chemical mechanisms underlying the transition from reversible bacterial adhesion to less reversible adhesion to substratum surfaces. (A) Bond-strengthening due to progressive removal of interfacial water, conformational changes in proteins, and re-arrangement of bacteria to expose favorable adhesion sites, like e.g. tufts of fibrils, towards a substratum surface. (B) Over the course of time, more reversibly binding tethers couple a bacterium irreversibly with a substratum surface. Since multiple reversibly binding tethers will not simultaneously detach, increasing numbers of binding tethers cause irreversible adhesion of an entire bacterium. (C) During bond-strengthening, surface appendages may collapse on a substratum surface to create more irreversible adhesion. (D) Examples of different retract AFM force-distance curves of type IV piliated P. aeruginosa. Collapse of individual pili results in plateaus adhesion force upon retract, due to gradual "peeling" of the tether from the substratum surface until fully peeled off (indicated in the insert). Reproduced from [120] with permission of the publisher, American Chemical Society.

studies (Fig. 4H), have indicated that over time more tethers become involved in adhesion of a bacterium (Fig. 5B). This does not necessarily imply a larger contact area between the cell wall of an adhering bacteria and a substratum surface [121], until the time when cell surface tethers involved in adhesion or EPS material attached to the cell wall have collapsed (see Section 4.2.3 below). Important evidence of the involvement of bacterial surface tethers in adhesion stems from adhesion of an engineered *E. coli* strain, in which the degree of fimbriation could be tuned without modification of its surface free energy or zeta potential, showing enhanced ability to adhere to substratum surfaces upon increasing the number of fimbriated tethers [122].

In AFM retraction force-distance curves, the number of minor adhesion forces [41] increases over time, suggesting multiple tether binding [82,90]. With the progressive involvement of more tethers in attaching bacteria to a surface, bacterial adhesion essentially becomes irreversible although single tethers may detach, which they will but are unlikely to do all at the same time [41]. Therewith, the tether-binding model of bacterial adhesion presents analogies with protein adsorption models. Proteins adsorb on surfaces through multiple, reversibly-adsorbed molecular segments [123]. Larger proteins can establish more molecular segments in contact with with the surface, increasing the unlikeliness of a simultaneous detachment of all molecular segments, compared to smaller proteins (forming the basis of the so-called "Vroman effect" for the irreversible displacement of adsorbed small blood proteins from a surface by larger molecular weight ones) [124]. As adsorption of large proteins is more irreversible than in small proteins, the increasing number of tethers will enhance the irreversibility of microbial adhesion through a similar mechanism.

4.2.3. Tether-collapse

Collapse of surface tethers of adhering bacteria to QCM-D crystal surfaces over time (Fig. 5C) [80] has been concluded from resident-time dependent dissipation monitoring according to Eq. 6. Streptococci with surface tethers, but not inert colloidal particles, showed decreases in dissipation shift that have been interpreted in terms of tether collapse and removal of interfacial water [80], similar as in protein adsorption studies with QCM-D [125,126]. The collapse of a surface tether will provide a larger contact area with the surface, that will increase the adhesion force and yields an elongated force plateau in retract AFM force-distance curves (Fig. 5D), due to gradual "peeling" of the collapsed tether from a substratum surface [120,127]. Tether collapse therewith contributes to more irreversible adhesion, contrary to extended tethers that convey higher mobility to an adhering bacterium and place it further away from the substratum surface, and depending on conditions, exposing it to higher fluid shear, which may lead to enhanced detachment [128].

5. Cell wall deformation and emergent biofilm properties

Nanoscopic cell wall deformation occurs in bacteria that are in direct contact with a substratum surface and is due to the adhesion forces felt by initially adhering bacteria as arising from the substratum surface (Fig. 6). Adhesion forces continue to deform a bacterial cell wall until balanced by the counterforces arising from the rigid peptidoglycan layer surrounding the cytoplasm and the intracellular pressure of the cytoplasm itself. Interestingly, until balanced, deformation increases the adhesion force because deformation brings more molecules, including molecules in the cytoplasm, closer to the substratum surface therewith enhancing their pair-wise molecular interaction with substratum molecules. Therewith, long-range Lifshitz-Van der Waals attractive forces [129] increase. In this perspective, cell wall deformation can be considered as another physico-chemical bond strengthening mechanism.

Adhesion force-sensing and associated cell wall deformation can make bacteria aware of the presence of a substratum surface and their adhering state through changes in lipid membrane surface tension to which membrane-located sensor molecules react to control emergent phenotypic and genotypic properties in biofilms [130]. Since adhering bacteria, depending on circumstances, block a much larger substratum surface area than their own geometric surface area (see Section 2), their number is relatively low and accordingly they must have means available to spread the information on the presence of a substratum surface and their adhering state to other bacteria in a biofilm. The bacterial reaction to direct adhesion-force sensing can be transmitted to other bacteria in the biofilm through quorum sensing, a communication system based on production and sensing of molecular autoinducers [131]. The "calling" distance over which bacteria can communicate through quorum sensing can vary widely between 5 [132] and 200 μm [133], depending on the autoinducer diffusion ability, adsorption to matrix components and the autoinducer threshold concentration required to obtain a response. Since under natural conditions, biofilms can reach thicknesses larger than 300 μm [10,11], adhesion-force sensing can generally be transmitted only to a limited number of bacterial layers close to the surface. Bacteria responding to molecular autoinducers will display emergent biofilm properties similar to as done by the initially adhering bacteria in direct contact with a substratum surface (Fig. 7) [25]. Therewith emergent properties are spread through a biofilm.

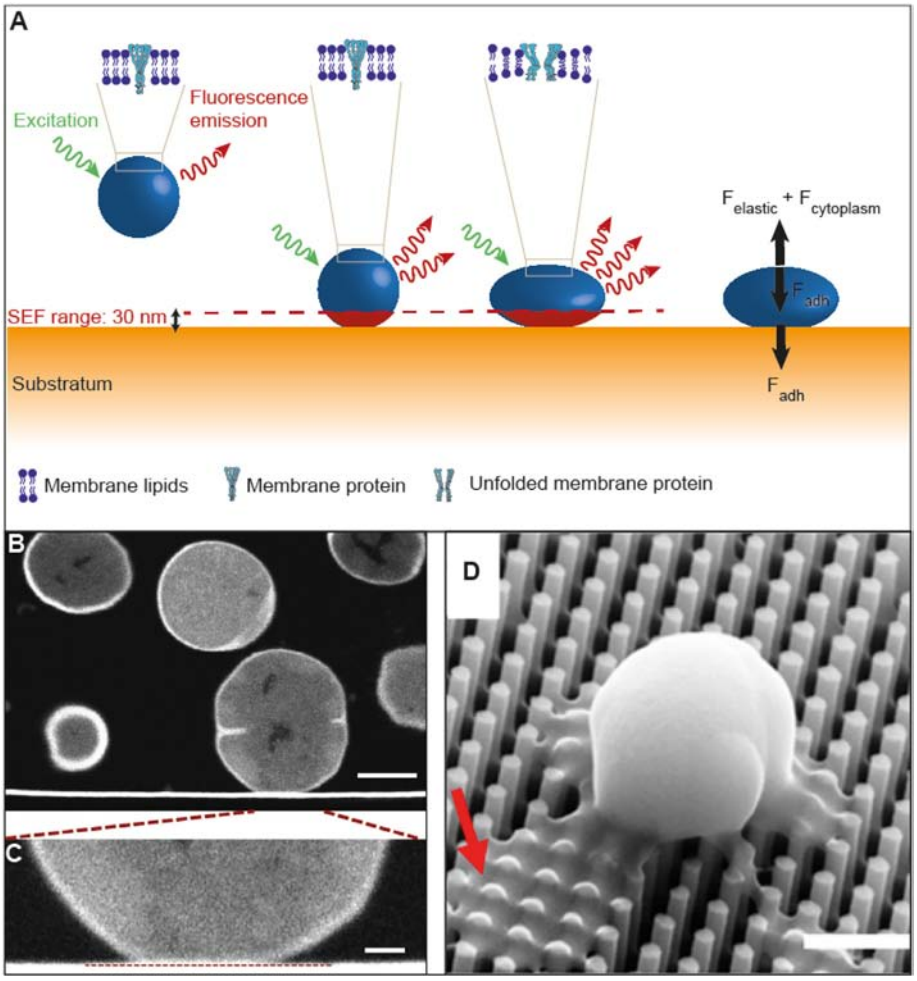

Fig. 6. Schematic presentation of surface enhanced fluorescence (SEF), cell wall deformation with associated surface tension changes in the cytoplasmic membrane, and forces acting on a deformed bacterium adhering on a surface. (A) Planktonic bacteria are too far above the substratum surface beyond the SEF range (30 nm) and no fluorescence enhancement is recorded. Upon adhesion to a (metal-reflecting) surface, a small portion of the fluorescent bacterium enters the range of SEF. Cell wall deformation due to adhesion forces brings more fluorophores within the bacterium within the SEF range, increasing fluorescence enhancement. Cell wall deformation in adhering bacteria is accompanied by membrane surface tension changes, due to reduced lipid density provoking hydrophobic mismatch and re-arrangement of membrane-located proteins. Adhesion forces (F_{adh}) between adhering bacteria and surfaces deform the cell wall until balanced by elastic counterforces arising from the rigid peptidoglycan layer ($F_{elastic}$) and the intracellular pressure of the cytoplasm itself ($F_{cytoplasm}$). (B, C) Backscattered SEM micrographs of a cross-section of a deformed S. aureus bacterium, adhering on a gold surface. Scale bar indicates 500 nm and 100 nm in panels B and C, respectively. Adapted from [134] with permission of the publisher, Royal Society of Chemistry. (D) SEM micrograph of S. aureus after being compressed between two nanopillared surfaces. Arrows indicate pressure-induced EPS production. Scale bar indicates 500 nm. Reproduced from [105] with permission of publisher, American Chemical Society.

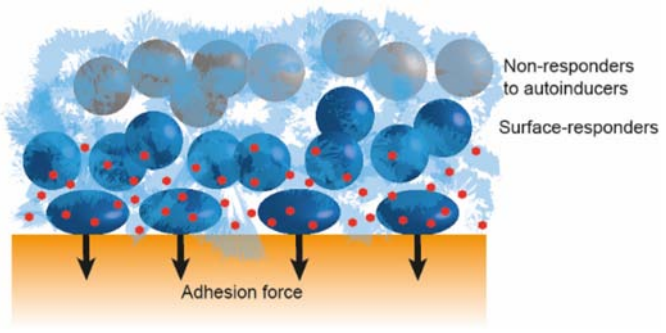

Fig. 7. Emergent properties of biofilms surface-programmed by adhesion forces. Physico-chemical properties of a substratum surface affect the forces by which the first layer of bacteria in contact with the surface adheres and therewith their cell wall deformation yields surface programmed-growth with emergent properties. Through sending out intra-biofilm signals, like quorum-sensing molecules or EPS by bacteria in direct contact with the substratum surface, also bacteria in a biofilm more remote from the surface respond with emergent properties. With increasing separation distances from the surface, the concentration of such autoinducers becomes insufficient to spread the word on adhesion-force sensing to all bacteria by means of quorum-sensing, and non-responders do not display surface-programmed emergent properties.

5.1. Extent of cell wall deformation in adhering bacteria

Unlike the microscopically visible deformation of mammalian cells upon adhesion to a surface [24] lacking a rigid peptidoglycan layer, adhering bacteria display nanoscopic cell wall deformations that have long remained unnoticed due to lack of experimental possibilities to visualize and quantify such small deformations.

Peak-force quantitative nanomechanical mapping AFM clearly visualized height reductions upon adhesion in *S. aureus*. The role of the peptidoglycan layer in maintaining bacterial shape upon adhesion follows from the much larger cell wall deformations observed in Δ*pbp4* mutants, lacking crosslinking of their peptidoglycan and that amounted up to 200 nm [129]. Focused-Ion-Beam tomography in combination with backscattered scanning electron microscopy (SEM) in *S. aureus* adhering to hydrophilic and hydrophobic surfaces also yielded direct visualization of cell wall deformations in *S. aureus* of between 30 nm to 100 nm [134], corresponding with AFM observations (Fig. 6B and C).

Microscopic methods, however, are time-consuming to analyze cell wall deformation in adhering bacteria. Surface enhanced fluorescence (SEF) can be used as an alternative that can measure adhering bacteria

over a surface area up to several tens of square centimeters depending on the substratum surface and camera system employed, but as a drawback does not yield direct visualization and requires fluorescent bacteria and reflective, metal substratum surfaces. SEF is the fluorescence increase taking place once a fluorophore is in close proximity to a reflective, metal surface [135] and decreases exponentially with increasing distance from the surface, becoming negligible at distances >30 nm above the surface [136]. In the case of fluorescent bacteria, fluorescence enhancement relative to the fluorescence of planktonic bacteria is recorded upon bacterial adhesion and cell wall deformation, which bring more fluorophores within the bacterium in the range of SEF (Fig. 6A) [23]. SEF can be done real-time during adhesion and has shown that cell wall deformation is residence-time dependent and it increases until reaching a maximum value of about 100–150 nm after 3 h upon first contact of a bacterium with the surface [23]. SEF has also shown that EPS around an adhering bacterium may act as a "cushion" to temporarily delay cell wall deformation after first contact until the EPS that tethers the bacterium to the surfaces has collapsed. Moreover, SEF has confirmed the role of peptidoglycan in maintaining bacterial shape upon adhesion while demonstrating cell wall weakening upon exposure of adhering *S. aureus* to antibiotics [137,138]. Also other environmental factors, like ionic strength variations [139] have been found to affect cell wall deformation.

5.2. Adhesion-induced emergent properties in biofilms

5.2.1. EPS production

While initial bond strengthening is a purely physico-chemical process taking place in both bacteria and abiotic colloidal particles, EPS production upon bacterial adhesion to surfaces is a biological process that contributes to strengthening of the bacterium-substratum bond. Adhesion has been described to stimulate EPS production in *C. crescentus* [140], while in *P. aeruginosa*, adhesion forces acting on pili induced gene expression changes and EPS production within 1–2 h after surface contact [141,142]. In 3–24 h old *S. aureus* biofilms, production of eDNA and poly-*N*-acetylglucosamine (PNAG), and the expression of genes responsible for their production, decreased with increasing adhesion forces [143], suggesting that bond-strengthening through EPS production only occurs according to environmental need to maintain an adhering state, i.e. in the absence of strong adhesion forces. A relation between production of EPS components and gene expression with adhesion forces was not observed in 1 h old biofilms, showing that time is required to spread information on adhesion forces from the initial colonizers to other bacterial layers [143]. Also for a Δ*pbp4* mutant, relations between production of EPS components and gene expression with adhesion forces were not observed, and accordingly intact peptidoglycan may be considered pivotal for adhesion force-sensing [143]. Bacteria adhering to nanopillared surfaces will experience high local stresses on the cell wall, that yield pressure-induced production of increased amounts of EPS [105] (Fig. 6D) that is transported towards the outer bacterial cell surface through membrane efflux pumps [144,145], in addition to other ways of release such as through secretion of membrane vesicles [146].

5.2.2. Efflux pumps

Efflux pumps also play a crucial role in removing antibiotic molecules from the cytoplasm and contribute to antibiotic tolerance [147]. Efflux pump activation follows chemical stress sensing by proteins located on the cytoplasmic membrane, but it is also dependent on surface adhesion. Upon exposure of *S. aureus* to nisin, activation of the two-component efflux system NsaRS, composed of an intra-membrane located histidine kinase NsaS and a response regulator NsaR, resulted in higher activation of the efflux pump NsaAB upon adhesion to surfaces generating stronger adhesion forces, concurrent with a higher antibiotic tolerance [148].

5.2.3. Mechano-sensitive channel gating

Mechano-sensitive channels can be formed by proteins located in the cytoplasmic membrane that enable bacterial exchange with the environment. Gating of mechano-sensitive channels occurs as a result of membrane surface tension changes [149–151] due hydrophobic mismatches in the membrane [150,152], after for instance a hypo-osmotic shock [153–155]. Opening of mechano-sensitive channels then allows water flow across the membrane to compensate for the undesirable changes in ionic strength. However, cell wall deformation due to adhesion can also generate changes in membrane surface tension, and it has been hypothesized that adhesion can also trigger mechano-sensitive channel gating, as part of the bacteria awareness of their adhering state on a surface [156].

5.3. Biofilm properties not induced by adhesion

Gene expression in biofilms is not controlled for all genes by the presence of a substratum surface and adhesion forces. Expression of *cidA* in *S. aureus* for instance [143], a gene regulating apoptosis according to oxidation and reduction conditions of the cytoplasmic membrane [157,158], did not relate with adhesion forces. Although adhesion force controlled gene expression is in its infancy, this suggests that only genes directly involved in bacterial adhesion to a substratum surface are expressed under the influence of substratum surface to which they adhere.

6. Conclusion

This review uniquely demonstrates that the impact of physical-chemistry on biofilm formation ranges from initial bacterial adhesion to what we propose here to call "surface-programmed" biofilm growth, to indicate the role of the substratum surface in the development of emergent biofilm properties. Unfortunately due to the huge variability in different bacterial strains and species and the enormous battery of adhesion mechanisms they have at their disposal, physico-chemical models of bacterial adhesion and biofilm formation have not advanced to possess predictive power and their current use is confined to "understanding in hindsight". Yet, for the initial stages of biofilm formation, such as bacterial mass transport and the transition from reversible to irreversible adhesion, comparison of bacterial behavior with colloidal particles indicates a pivotal role of bacterial cell surface tethers. Nanoscopic cell wall deformation in response to adhesion forces felt by initially adhering bacteria in direct contact with the substratum surface, controls emergent phenotypic and genotypic properties in biofilms. Therewith physico-chemistry explains many more aspects of biofilm formation, that have hitherto only been attributed to the microbiological domain. This conclusion is pivotal for the development of new strategies to control biofilm formation through modification of substratum surfaces, that have long focused on initial bacterial adhesion phenomena.

Acknowledgments

This study was entirely funded by the University Medical Center Groningen, Groningen, The Netherlands. H.J.B. is also a director of a consulting company, SASA BV. We declare no potential conflicts of interest with respect to authorship and/or publication of this article. The opinions and assertions contained herein are those of the authors and are not construed as necessarily representing the views of the funding organization or the authors' employers.

References

[1] Enning D, Garrelfs J. Corrosion of iron by sulfate-reducing bacteria: new views of an old problem. Appl Environ Microbiol 2014;80:1226–36. https://doi.org/10.1128/AEM.02848-13.

[2] Bain R, Cronk R, Hossain R, Bonjour S, Onda K, Wright J, et al. Global assessment of exposure to faecal contamination through drinking water based on a systematic review. Trop Med Int Health 2014;19:917–27. https://doi.org/10.1111/tmi.12334.

[3] Simón-Soro A, Mira A. Solving the etiology of dental caries. Trends Microbiol 2015; 23:76–82. https://doi.org/10.1016/j.tim.2014.10.010.

[4] Raphel J, Holodniy M, Goodman SB, Heilshorn SC. Multifunctional coatings to simultaneously promote osseointegration and prevent infection of orthopaedic implants. Biomaterials 2016;84:301–14. https://doi.org/10.1016/j.biomaterials.2016.01.016.

[5] Riool M, De Boer L, Jaspers V, Van der Loos CM, Van Wamel WJB, Wu G, et al. *Staphylococcus epidermidis* originating from titanium implants infects surrounding tissue and immune cells. Acta Biomater 2014;10:5202–12. https://doi.org/10.1016/j.actbio.2014.08.012.

[6] Cycoń M, Piotrowska-Seget Z. Pyrethroid-degrading microorganisms and their potential for the bioremediation of contaminated soils: a review. Front Microbiol 2016;7:1463. https://doi.org/10.3389/fmicb.2016.01463.

[7] Li J, Sung CYJ, Lee N, Ni Y, Pihlajamäki J, Panagiotou G, et al. Probiotics modulated gut microbiota suppresses hepatocellular carcinoma growth in mice. Proc Natl Acad Sci 2016;113:E1306–15. https://doi.org/10.1073/pnas.1518189113.

[8] Pamer EG. Resurrecting the intestinal microbiota to combat antibiotic-resistant pathogens. Science 2016;352:535–8. https://doi.org/10.1126/science.aad9382 (80-).

[9] Li J, Busscher HJ, Norde W, Sjollema J. Analysis of the contribution of sedimentation to bacterial mass transport in a parallel plate flow chamber. Colloids Surf B Biointerfaces 2011;84:76–81. https://doi.org/10.1016/j.colsurfb.2010.12.018.

[10] Jang A, Szabo J, Hosni AA, Coughlin M, Bishop PL. Measurement of chlorine dioxide penetration in dairy process pipe biofilms during disinfection. Appl Microbiol Biotechnol 2006;72:368–76. https://doi.org/10.1007/s00253-005-0274-5.

[11] Klein MI, Hwang G, Santos PHS, Campanella OH, Koo H. *Streptococcus mutans*-derived extracellular matrix in cariogenic oral biofilms. Front Cell Infect Microbiol 2015;5:10. https://doi.org/10.3389/fcimb.2015.00010.

[12] Sjollema J, Rustema-Abbing M, Van der Mei HC, Busscher HJ. Generalized relationship between numbers of bacteria and their viability in biofilms. Appl Environ Microbiol 2011;77:5027–9. https://doi.org/10.1128/AEM.00178-11.

[13] Flemming HC, Wingender J, Szewzyk U, Steinberg P, Rice SA, Kjelleberg S. Biofilms: an emergent form of bacterial life. Nat Rev Microbiol 2016;14:563–75. https://doi.org/10.1038/nrmicro.2016.94.

[14] Palmer RJ, White DC. Developmental biology of biofilms: implications for treatment and control. Trends Microbiol 1997;5:435–40. https://doi.org/10.1016/S0966-842X(97)01142-6.

[15] Moreira JMR, Araújo JDP, Miranda JM, Simões M, Melo LF, Mergulhão FJ. The effects of surface properties on *Escherichia coli* adhesion are modulated by shear stress. Colloids Surf B Biointerfaces 2014;123:1–7. https://doi.org/10.1016/j.colsurfb.2014.08.016.

[16] Nuryastuti T, Krom BP. *Ica*-status of clinical *Staphylococcus epidermidis* strains affects adhesion and aggregation: a thermodynamic analysis. Antonie Van Leeuwenhoek 2017;110:1467–74. https://doi.org/10.1007/s10482-017-0899-2.

[17] Harimawan A, Zhong S, Lim C-T, Ting Y-P. Adhesion of *B. subtilis* spores and vegetative cells onto stainless steel - DLVO theories and AFM spectroscopy. J Colloid Interface Sci 2013;405:233–41. https://doi.org/10.1016/j.jcis.2013.05.031.

[18] Formosa-Dague C, Duval RE, Dague E. Cell biology of microbes and pharmacology of antimicrobial drugs explored by atomic force microscopy. Semin Cell Dev Biol 2018;73:165–76. https://doi.org/10.1016/j.semcdb.2017.06.022.

[19] Zakrisson J, Singh B, Svenmarker P, Wiklund K, Zhang H, Hakobyan S, et al. Detecting bacterial surface organelles on single cells using optical tweezers. Langmuir 2016;32:4521–9. https://doi.org/10.1021/acs.langmuir.5b03845.

[20] Wang Y, Narain R, Liu Y. Study of bacterial adhesion on different glycopolymer surfaces by quartz crystal microbalance with dissipation. Langmuir 2014;30:7377–87. https://doi.org/10.1021/la5016115.

[21] Eskhan AO, Abu-Lail NI. A new approach to decoupling of bacterial adhesion energies measured by AFM into specific and nonspecific components. Colloid Polym Sci 2014;292:343–53. https://doi.org/10.1007/s00396-013-3017-7.

[22] Xiao J, Dufrêne YF. Optical and force nanoscopy in microbiology. Nat Microbiol 2016;1:16186. https://doi.org/10.1038/NMICROBIOL.2016.186.

[23] Li J, Busscher HJ, Swartjes JJTM, Chen Y, Harapanahalli AK, Norde W, et al. Residence-time dependent cell wall deformation of different *Staphylococcus aureus* strains on gold measured using surface-enhanced-fluorescence. Soft Matter 2014; 10:7638–46. https://doi.org/10.1039/c4sm00584h.

[24] Santoro F, Zhao W, Joubert L-M, Duan L, Schnitker J, Van de Burgt Y, et al. Revealing the cell—material interface with nanometer resolution by focused ion beam/scanning electron microscopy. ACS Nano 2017;11:8320–8. https://doi.org/10.1021/acsnano.7b03494.

[25] Ren Y, Wang C, Chen Z, Allan E, Van der Mei HC, Busscher HJ. Emergent heterogeneous microenvironments in biofilms: substratum surface heterogeneity and bacterial adhesion force-sensing. FEMS Microbiol Rev 2018;42:259–72. https://doi.org/10.1093/femsre/fuy001.

[26] Drescher K, Dunkel J, Nadell CD, Van Teeffelen S, Grnja I, Wingreen NS, et al. Architectural transitions in *Vibrio cholerae* biofilms at single-cell resolution. Proc Natl Acad Sci 2016;113:E2066–72. https://doi.org/10.1073/pnas.1601702113.

[27] Sales-Ortells H, Medema G. Screening-level risk assessment of *Coxiella burnetii* (Q fever) transmission via aeration of drinking water. Environ Sci Technol 2012;46: 4125–33. https://doi.org/10.1021/es203744g.

[28] Gut IM, Bartlett RA, Yeager JJ, Leroux B, Ratnesar-Shumate S, Dabisch P, et al. Extraction of aerosol-deposited*Yersinia pestis* from indoor surfaces to determine bacterial environmental decay. Appl Environ Microbiol 2016;82:2809–18. https://doi.org/10.1128/AEM.03989-15.

[29] Vu K, Yang G, Wang B, Tawfiq K, Chen G. Bacterial interactions and transport in geological formation of alumino-silica clays. Colloids Surf B Biointerfaces 2015; 125:45–50. https://doi.org/10.1016/j.colsurfb.2014.11.015.

[30] Tran VB, Fleiszig SMJ, Evans DJ, Radke CJ. Dynamics of flagellum-and pilus-mediated association of *Pseudomonas aeruginosa* with contact lens surfaces. Appl Environ Microbiol 2011;77:3644–52. https://doi.org/10.1128/AEM.02656-10.

[31] Busscher HJ, Van der Mei HC. Microbial adhesion in flow displacement systems. Clin Microbiol Rev 2006;19:127–41. https://doi.org/10.1128/CMR.19.1.127-141.2006.

[32] Elimelech M. Particle deposition on ideal collectors from dilute flowing suspensions: mathematical formulation, numerical solution, and simulations. Sep Technol 1994;4:186–212. https://doi.org/10.1016/0956-9618(94)80024-3.

[33] Adamczyk Z, Van de Ven TGM. Deposition of particles under external forces in laminar flow through parallel-plate and cylindrical channels. J Colloid Interface Sci 1981;80:340–56. https://doi.org/10.1016/0021-9797(81)90193-4.

[34] Meinders JM, Van der Mei HC, Busscher HJ. Deposition efficiency and reversibility of bacterial adhesion under flow. J Colloid Interface Sci 1995;176:329–41. https://doi.org/10.1006/jcis.1995.9960.

[35] Seymour MB, Chen G, Su C, Li Y. Transport and retention of colloids in porous media: does shape really matter? Environ Sci Technol 2013;47:8391–8. https://doi.org/10.1021/es4016124.

[36] Chen G, Hong Y, Walker SL. Colloidal and bacterial deposition: role of gravity. Langmuir 2010;26:314–9. https://doi.org/10.1021/la903089x.

[37] Boks NP, Norde W, Van der Mei HC, Busscher HJ. Forces involved in bacterial adhesion to hydrophilic and hydrophobic surfaces. Microbiology 2008;154:3122–33. https://doi.org/10.1099/mic.0.2008/018622-0.

[38] Li J, Busscher HJ, Van der Mei HC, Norde W, Krom BP, Sjollema J. Analysis of the contribution of sedimentation to bacterial mass transport in a parallel plate flow chamber. Part II: use of fluorescence imaging. Colloids Surf B Biointerfaces 2011; 87:427–32. https://doi.org/10.1016/j.colsurfb.2011.06.002.

[39] Bakker DP, Van der Plaats A, Verkerke GJ, Busscher HJ, Van der Mei HC. Comparison of velocity profiles for different flow chamber designs used in studies of microbial adhesion to surfaces. Appl Environ Microbiol 2003;69:6280–7. https://doi.org/10.1128/AEM.69.10.6280-6287.2003.

[40] De Kerchove AJ, Elimelech M. Bacterial swimming motility enhances cell deposition and surface coverage. Environ Sci Technol 2008;42:4371–7. https://doi.org/10.1021/es703028u.

[41] Sjollema J, Van der Mei HC, Hall CL, Peterson BW, De Vries J, Song L, et al. Detachment and successive re- attachment of multiple, reversibly- binding tethers result in irreversible bacterial adhesion to surfaces. Sci Rep 2017;7:4369. https://doi.org/10.1038/s41598-017-04703-8.

[42] Wang H, Sodagari M, Chen Y, He X, Zhang Newby B-M, Ju L-K. Initial bacterial attachment in slow flowing systems: effects of cell and substrate surface properties. Colloids Surf B Biointerfaces 2011;87:415–22. https://doi.org/10.1016/j.colsurfb.2011.05.053.

[43] Sharma S, Jaimes-Lizcano YA, Mclay RB, Cirino PC, Conrad JC. Subnanometric roughness affects the deposition and mobile adhesion of *Escherichia coli* on silanized glass surfaces. Langmuir 2016;32:5422–33. https://doi.org/10.1021/acs.langmuir.6b00883.

[44] Lu N, Bevard T, Massoudieh A, Zhang C, Dohnalkova AC, Zilles JL, et al. Flagella-mediated differences in deposition dynamics for *Azotobacter vinelandii* in porous media. Environ Sci Technol 2013;47:5162–70. https://doi.org/10.1021/es3053398.

[45] Rijnaarts HHM, Norde W, Bouwer EJ, Lyklema J, Zehnder AJB. Bacterial deposition in porous media related to the cleanbed collision efficiency and to substratum blocking by attached cells. Environ Sci Technol 1996;30:2869–76.

[46] Adamczyk Z, Siwek B, Zembala M, Belouschek P. Kinetics of localized adsorption of colloid particles. Adv Colloid Interface Sci 1994;48:151–280. https://doi.org/10.1016/0001-8686(94)80008-1.

[47] Ko C-H, Elimelech M. The "shadow effect" in colloid transport and deposition dynamics in granular porous media: measurements and mechanisms. Environ Sci Technol 2000;34:3681–9. https://doi.org/10.1021/es0009323.

[48] Camesano TA, Logan BE. Influence of fluid velocity and cell concentration on the transport of motile and nonmotile bacteria in porous media. Environ Sci Technol 1998;32:1699–708.

[49] Busscher HJ, Van der Mei HC. Use of flow chamber devices and image analysis methods to study microbial adhesion. Methods Enzymol 1995;253:455–77. https://doi.org/10.1016/S0076-6879(95)53039-8.

[50] Boks NP, Kaper HJ, Norde W, Busscher HJ, Van der Mei HC. Residence time dependent desorption of *Staphylococcus epidermidis* from hydrophobic and hydrophilic substrata. Colloids Surf B Biointerfaces 2008;67:276–8. https://doi.org/10.1016/j.colsurfb.2008.08.021.

[51] Busscher HJ, Uyen MHMJC, Weerkamp AH, Postma WJ, Arends J. Reversibility of adhesion of oral streptococci to solids. FEMS Microbiol Lett 1986;35:303–6.

[52] Mercier-Bonin M, Duviau M-P, Ellero C, Lebleu N, Raynaud P, Despax B, et al. Dynamics of detachment of *Escherichia coli* from plasma-mediated coatings under shear flow. Biofouling 2012;28:881–94. https://doi.org/10.1080/08927014.2012.719160.

[53] Khodaparast S, Kim MK, Silpe JE, Stone HA. Bubble-driven detachment of bacteria from confined microgeometries. Environ Sci Technol 2017;51:1340–7. https://doi.org/10.1021/acs.est.6b04369.

[54] Van der Mei HC, Busscher HJ. On the difference between water contact angles measured on partly dehydrated and on freeze-dried oral streptococci. J Colloid Interface Sci 1990;136:297–300.

[55] Absolom DR, Lamberti FV, Policova Z, Zingg W, Van Oss CJ, Neumann AW. Surface thermodynamics of bacterial adhesion. Appl Environ Microbiol 1983;46:90–7.

[56] Vilinska A, Rao KH. Surface thermodynamics and extended DLVO theory of *Leptospirillum ferrooxidans* cells' adhesion on sulfide minerals. Miner Metall Process 2011;28:151–8.
[57] Katsikogianni MG, Missirlis YF. Bacterial adhesion onto materials with specific surface chemistries under flow conditions. J Mater Sci Mater Med 2010;21:963–8. https://doi.org/10.1007/s10856-009-3975-y.
[58] Feng W, Swift S, Singhal N. Effects of surfactants on cell surface tension parameters and hydrophobicity of *Pseudomonas putida* 852 and *Rhodococcus erythropolis* 3586. Colloids Surf B Biointerfaces 2013;105:43–50. https://doi.org/10.1016/j.colsurfb.2012.12.034.
[59] Pimentel-Filho NJ, Martins MC, Nogueira GB, Mantovani HC, Vanetti MC. Bovicin HC5 and nisin reduce *Staphylococcus aureus* adhesion to polystyrene and change the hydrophobicity profile and Gibbs free energy of adhesion. Int J Food Microbiol 2014;190:1–8. https://doi.org/10.1016/j.ijfoodmicro.2014.08.004.
[60] Van der Westen R, Sjollema J, Molenaar R, Sharma PK, Van der Mei HC, Busscher HJ. Floating and tether-coupled adhesion of bacteria to hydrophobic and hydrophilic surfaces. Langmuir 2018;34:4937–44. https://doi.org/10.1021/acs.langmuir.7b04331.
[61] Van der Mei HC, Handley PS, Busscher HJ. Depth profiling of the elemental surface composition of the oral microorganism S. salivarius HB and fibrillar mutants by X-ray photoelectron spectroscopy. Cell Biochem Biophys 1992;20:99–110. https://doi.org/10.1007/BF02782657.
[62] Munera D, Palomino C, Fernández LÁ. Specific residues in the N-terminal domain of FimH stimulate type 1 fimbriae assembly in *Escherichia coli* following the initial binding of the adhesin to FimD usher. Mol Microbiol 2008;69:911–25. https://doi.org/10.1111/j.1365-2958.2008.06325.x.
[63] Van Oss CJ, Good RJ, Chaudhury MK. The role of Van der Waals forces and hydrogen bonds in "hydrophobic interactions" between biopolymers and low energy surfaces. J Colloid Interface Sci 1986;111:378–90. https://doi.org/10.1016/0021-9797(86)90041-X.
[64] Bos R, Van der Mei HC, Busscher HJ. Physico-chemistry of initial microbial adhesive interactions – its mechanisms and methods for study. FEMS Microbiol Rev 1999;23:179–230. https://doi.org/10.1016/S0168-6445(99)00004-2.
[65] Jucker BA, Harms H, Zehnder AJ. Adhesion of the positively charged bacterium *Stenotrophomonas* (*Xanthomonas*) *maltophilia* 70401 to glass and Teflon. J Bacteriol 1996;178:5472–9. https://doi.org/10.1128/jb.178.18.5472-5479.1996.
[66] Spriano S, Sarath Chandra V, Cochis A, Uberti F, Rimondini L, Bertone E, et al. How do wettability, zeta potential and hydroxylation degree affect the biological response of biomaterials? Mater Sci Eng C 2017;74:542–55. https://doi.org/10.1016/j.msec.2016.12.107.
[67] Wang L-L, Wang L-F, Ren X-M, Ye X-D, Li W-W, Yuan S-J, et al. pH dependence of structure and surface properties of microbial EPS. Environ Sci Technol 2012;46:737–44. https://doi.org/10.1021/es203540w.
[68] Feng G, Cheng Y, Wang SY, Hsu LC, Feliz Y, Borca-Tasciuc DA, et al. Alumina surfaces with nanoscale topography reduce attachment and biofilm formation by *Escherichia coli* and *Listeria* spp. Biofouling 2014;30:1253–68. https://doi.org/10.1080/08927014.2014.976561.
[69] Kumar A, Ting Y-P. Effect of sub-inhibitory antibacterial stress on bacterial surface properties and biofilm formation. Colloids Surf B Biointerfaces 2013;111:747–54. https://doi.org/10.1016/j.colsurfb.2013.07.011.
[70] Fletcher M. Effects of electrolytes on attachment of aquatic bacteria to solid Surfaces. Estuaries 1988;11:226–30.
[71] Hermansson M. The DLVO theory in microbial adhesion. Colloids Surf B Biointerfaces 1999;14:105–19. https://doi.org/10.1016/S0927-7765(99)00029-6.
[72] Nguyen V, Karunakaran E, Collins G, Biggs CA. Physicochemical analysis of initial adhesion and biofilm formation of *Methanosarcina barkeri* on polymer support material. Colloids Surf B Biointerfaces 2016;143:518–25. https://doi.org/10.1016/j.colsurfb.2016.03.042.
[73] Ostvar S, Wood BD. Multiscale model describing bacterial adhesion and detachment. Langmuir 2016;32:5213–22. https://doi.org/10.1021/acs.langmuir.6b00882.
[74] Bruzaud J, Tarrade J, Coudreuse A, Canette A, Herry J-M, Taffin De Givenchy E, et al. Flagella but not type IV pili are involved in the initial adhesion of *Pseudomonas aeruginosa* PAO1 to hydrophobic or superhydrophobic surfaces. Colloids Surf B Biointerfaces 2015;131:59–66. https://doi.org/10.1016/j.colsurfb.2015.04.036.
[75] Sharma S, Conrad JC. Attachment from flow of *Escherichia coli* bacteria onto silanized glass substrates. Langmuir 2014;30:11147–55. https://doi.org/10.1021/la502313y.
[76] Dabros T, Warszynski P, Van de Ven TGM. Motion of latex spheres tethered to a surface. J Colloid Interface Sci 1994;162:254–6. https://doi.org/10.1006/jcis.1994.1034.
[77] Chao Y, Zhang T. Probing roles of lipopolysaccharide, type 1 fimbria, and colanic acid in the attachment of *Escherichia coli* strains on inert surfaces. Langmuir 2011;27:11545–53. https://doi.org/10.1021/la202534p.
[78] Pranzetti A, Mieszkin S, Iqbal P, Rawson FJ, Callow ME, Callow JA, et al. An electrically reversible switchable surface to control and study early bacterial adhesion dynamics in real-time. Adv Mater 2013;25:2181–5. https://doi.org/10.1002/adma.201204880.
[79] Fang B, Jiang Y, Rotello VM, Nüsslein K, Santore MM. Easy come easy go: surfaces containing immobilized nanoparticles or isolated polycation chains facilitate removal of captured *Staphylococcus aureus* by retarding bacterial bond maturation. ACS Nano 2014;8:1180–90. https://doi.org/10.1021/nn405845y.
[80] Olsson ALJ, Van der Mei HC, Busscher HJ, Sharma PK. Novel analysis of bacterium-substratum bond maturation measured using a quartz crystal microbalance. Langmuir 2010;26:11113–7. https://doi.org/10.1021/la100896a.
[81] Zeng G, Müller T, Meyer RL. Single-cell force spectroscopy of bacteria enabled by naturally derived proteins. Langmuir 2014;30:4019–25. https://doi.org/10.1021/la404673q.
[82] Prystopiuk V, Feuillie C, Herman-Bausier P, Viela F, Alsteens D, Pietrocola G, et al. Mechanical forces guiding *Staphylococcus aureus* cellular invasion. ACS Nano 2018;12:3609–22. https://doi.org/10.1021/acsnano.8b00716.
[83] Xu L-C, Vadillo-Rodriguez V, Logan BE. Residence time, loading force, pH, and ionic strength affect adhesion forces between colloids and biopolymer-coated surfaces. Langmuir 2005;21:7491–500. https://doi.org/10.1021/la0509091.
[84] Olsson ALJ, Mitzel MR, Tufenkji N. QCM-D for non-destructive real-time assessment of *Pseudomonas aeruginosa* biofilm attachment to the substratum during biofilm growth. Colloids Surf B Biointerfaces 2015;136:928–34. https://doi.org/10.1016/j.colsurfb.2015.10.032.
[85] Wong KKW, Olsson ALJ, Asadishad B, Van der Bruggen B, Tufenkji N. Role of cell appendages in initial attachment and stability of *E coli* on silica monitored by nondestructive TIRF microscopy. Langmuir 2017;33:4066–75. https://doi.org/10.1021/acs.langmuir.7b00314.
[86] Dabros T, Van de Ven TGM. Kinetics of coating by colloidal particles. J Colloid Interface Sci 1982;89:232–44.
[87] Fredriksson C, Kihlman S, Rodahl M, Kasemo B. The piezoelectric quartz crystal mass and dissipation sensor: a means of studying cell adhesion. Langmuir 1997;14:248–51. https://doi.org/10.1021/la9710051.
[88] Wang KF, Nagarajan R, Camesano TA. Antimicrobial peptide alamethicin insertion into lipid bilayer: a QCM-D exploration. Colloids Surf B Biointerfaces 2014;116:472–81. https://doi.org/10.1016/j.colsurfb.2014.01.036.
[89] Boks NP, Busscher HJ, Van der Mei HC, Norde W. Bond-strengthening in staphylococcal adhesion to hydrophilic and hydrophobic surfaces using atomic force microscopy. Langmuir 2008;24:12990–4. https://doi.org/10.1021/la801824c.
[90] Formosa-Dague C, Feuillie C, Beaussart A, Derclaye S, Kucharíkova S, Lasa I, et al. Sticky matrix: adhesion mechanism of the staphylococcal polysaccharide intercellular adhesin. ACS Nano 2016;10:3443–52. https://doi.org/10.1021/acsnano.5b07515.
[91] Mei L, Ren Y, Busscher HJ, Chen Y, Van der Mei HC. Poisson analysis of streptococcal bond-strengthening on saliva-coated enamel. J Dent Res 2009;88:841–5. https://doi.org/10.1177/0022034509342523.
[92] Abu-Lail NI, Camesano TA. Specific and nonspecific interaction forces between *Escherichia coli* and silicon nitride, determined by Poisson statistical analysis. Langmuir 2006:7296–301. https://doi.org/10.1021/la0533415.
[93] Chen Y, Busscher HJ, Van der Mei HC, Norde W. Statistical analysis of long-and short-range forces involved in bacterial adhesion to substratum surfaces as measured using atomic force microscopy. Appl Environ Microbiol 2011;77:5065–70. https://doi.org/10.1128/AEM.00502-11.
[94] Xing SF, Sun XF, Taylor AA, Walker SL, Wang YF, Wang SG. D-Amino acids inhibit initial bacterial adhesion: thermodynamic evidence. Biotechnol Bioeng 2015;112:696–704. https://doi.org/10.1002/bit.25479.
[95] Cho N-J, Frank CW, Kasemo B, Höök F. Quartz crystal microbalance with dissipation monitoring of supported lipid bilayers on various substrates. Nat Protoc 2010;5:1096–106. https://doi.org/10.1038/nprot.2010.65.
[96] Huang Q, Wu H, Cai P, Fein JB, Chen W. Atomic force microscopy measurements of bacterial adhesion and biofilm formation onto clay-sized particles. Sci Rep 2015;5:16857. https://doi.org/10.1038/srep16857.
[97] Schneckenburger H. Total internal reflection fluorescence microscopy: technical innovations and novel applications. Curr Opin Biotechnol 2005;16:13–8. https://doi.org/10.1016/j.copbio.2004.12.004.
[98] Lecuyer S, Rusconi R, Shen Y, Forsyth A, Vlamakis H, Kolter R, et al. Shear stress increases the residence time of adhesion of *Pseudomonas aeruginosa*. Biophys J 2011;100:341–50. https://doi.org/10.1016/j.bpj.2010.11.078.
[99] Hoffman MD, Zucker LI, Brown PJB, Kysela DT, Brun YV, Jacobson SC. Timescales and frequencies of reversible and irreversible adhesion events of single bacterial cells. Anal Chem 2015;87:12032–9. https://doi.org/10.1021/acs.analchem.5b02087.
[100] Xu C-P, Boks NP, De Vries J, Kaper HJ, Norde W, Busscher HJ, et al. *Staphylococcus aureus*-fibronectin interactions with and without fibronectin-binding proteins and their role in adhesion and desorption. Appl Environ Microbiol 2008;74:7522–8. https://doi.org/10.1128/AEM.00948-08.
[101] Gutman J, Walker SL, Freger V, Herzberg M. Bacterial attachment and viscoelasticity: physicochemical and motility effects analyzed using quartz crystal microbalance with dissipation (QCM-D). Environ Sci Technol 2013;47:398–404. https://doi.org/10.1021/es303394w.
[102] Das T, Sharma PK, Krom BP, Van der Mei HC, Busscher HJ. Role of eDNA on the adhesion forces between *Streptococcus mutans* and substratum surfaces: influence of ionic strength and substratum hydrophobicity. Langmuir 2011;27:10113–8. https://doi.org/10.1021/la202013m.
[103] Potthoff E, Ossola D, Zambelli T, Vorholt JA. Bacterial adhesion force quantification by fluidic force microscopy. Nanoscale 2015;7:4070–9. https://doi.org/10.1039/c4nr06495j.
[104] Harimawan A, Rajasekar A, Ting Y-P. Bacteria attachment to surfaces – AFM force spectroscopy and physicochemical analyses. J Colloid Interface Sci 2011;364:213–8. https://doi.org/10.1016/j.jcis.2011.08.021.
[105] Hizal F, Choi C-H, Busscher HJ, Van der Mei HC. Staphylococcal adhesion, detachment and transmission on nanopillared Si surfaces. Appl Mater Interfaces 2016;8:30430–9. https://doi.org/10.1021/acsami.6b09437.
[106] Vadillo-Rodríguez V, Busscher HJ, Norde W, De Vries J, Van der Mei HC. Atomic force microscopic corroboration of bond aging for adhesion of *Streptococcus thermophilus* to solid substrata. J Colloid Interface Sci 2004;278:251–4. https://doi.org/10.1016/j.jcis.2004.05.045.
[107] Le DT, Guérardel Y, Loubière P, Mercier-Bonin M, Dague E. Measuring kinetic dissociation/association constants between *Lactococcus lactis* bacteria and mucins using living cell probes. Biophys J 2011;101:2843–53. https://doi.org/10.1016/j.bpj.2011.10.034.

[108] Xu L-C, Logan BE. Interaction forces measured using AFM between colloids and surfaces coated with both dextran and protein. Langmuir 2006;22:4720–7. https://doi.org/10.1021/la053443v.
[109] Younes JA, Van der Mei HC, Van den Heuvel E, Busscher HJ, Reid G. Adhesion forces and coaggregation between vaginal staphylococci and lactobacilli. PLoS One 2012;7:e36917. https://doi.org/10.1371/journal.pone.0036917.
[110] Das T, Krom BP, Van der Mei HC, Busscher HJ, Sharma PK. DNA-mediated bacterial aggregation is dictated by acid–base interactions. Soft Matter 2011;7:2927–35. https://doi.org/10.1039/c0sm01142h.
[111] Ovchinnikova ES, Krom BP, Harapanahalli AK, Busscher HJ, Van der Mei HC. Surface thermodynamic and adhesion force evaluation of the role of chitin-binding protein in the physical interaction between *Pseudomonas aeruginosa* and *Candida albicans*. Langmuir 2013;29:4823–9. https://doi.org/10.1021/la400554g.
[112] Aguayo S, Donos N, Spratt D, Bozec L. Probing the nanoadhesion of *Streptococcus sanguinis* to titanium implant surfaces by atomic force microscopy. Int J Nanomedicine 2016;11:1443–50. https://doi.org/10.2147/IJN.S100768.
[113] Hou J, Veeregowda DH, Van de Belt-Gritter B, Busscher HJ, Van der Mei HC. Extracellular polymeric matrix production and relaxation under fluid shear and mechanical pressure in *Staphylococcus aureus* biofilms. Appl Environ Microbiol 2017;84:e01516–7. https://doi.org/10.1128/AEM.01516-17.
[114] Das T, Sharma PK, Busscher HJ, Van der Mei HC, Krom BP. Role of extracellular DNA in initial bacterial adhesion and surface aggregation. Appl Environ Microbiol 2010;76:3405–8. https://doi.org/10.1128/AEM.03119-09.
[115] Norde W. My voyage of discovery to proteins in flatland ...and beyond. Colloids Surf B Biointerfaces 2008;61:1–9. https://doi.org/10.1016/j.colsurfb.2007.09.029.
[116] Busscher HJ, Norde W, Sharma PK, Van der Mei HC. Interfacial re-arrangement in initial microbial adhesion to surfaces. Curr Opin Colloid Interface Sci 2010;15:510–7. https://doi.org/10.1016/j.cocis.2010.05.014.
[117] Vitry P, Valotteau C, Feuillie C, Bernard S, Alsteens D, Geoghegan JA, et al. Force-induced strengthening of the interaction between *Staphylococcus aureus* clumping factor B and loricrin. MBio 2017;8. https://doi.org/10.1128/mBio.01748-17 e01748–17.
[118] Mouton C, Reynolds HS, Genco RJ. Characterization of tufted streptococci isolated from the "corn cob" configuration of human dental plaque. Infect Immun 1980;27:235–45.
[119] Kalasin S, Dabkowski J, Nüsslein K, Santore MM. The role of nano-scale heterogeneous electrostatic interactions in initial bacterial adhesion from flow: a case study with *Staphylococcus aureus*. Colloids Surf B Biointerfaces 2010;76:489–95. https://doi.org/10.1016/j.colsurfb.2009.12.009.
[120] Beaussart A, Baker AE, Kuchma SL, El-Kirat-Chatel S, O'Toole GA, Dufrêne YF. Nanoscale adhesion forces of *Pseudomonas aeruginosa* type IV pili. ACS Nano 2014;8:10723–33. https://doi.org/10.1021/nn5044383.
[121] Spengler C, Thewes N, Jung P, Bischoff M, Jacobs K. Determination of the nanoscaled contact area of staphylococcal cells. Nanoscale 2017;9:10084–93. https://doi.org/10.1039/c7nr02297b.
[122] McLay RB, Nguyen HN, Jaimes-Lizcano YA, Dewangan NK, Alexandrova S, Rodrigues DF, et al. Level of fimbriation alters the adhesion of *Escherichia coli* bacteria to interfaces. Langmuir 2017;34:1133–42. https://doi.org/10.1021/acs.langmuir.7b02447.
[123] Norde W, Haynes CA. Reversibility and the mechanism of protein adsorption. ACS Symp Ser 1995;602:26–40. https://doi.org/10.1021/bk-1995-0602.ch002.
[124] Vroman L. Finding seconds count after contact with blood (and that is all I did). Colloids Surf B Biointerfaces 2008;62:1–4. https://doi.org/10.1016/j.colsurfb.2007.11.017.
[125] Berglin M, Pinori E, Sellborn A, Andersson M, Hulander M, Elwing H. Fibrinogen adsorption and conformational change on model polymers: novel aspects of mutual molecular rearrangement. Langmuir 2009;25:5602–56028. https://doi.org/10.1021/la803686m.
[126] Vörös J. The density and refractive index of adsorbing protein layers. Biophys J 2004;87:553–61. https://doi.org/10.1529/biophysj.103.030072.
[127] Lu S, Giuliani M, Harvey H, Burrows LL, Wickham RA, Dutcher JR. Nanoscale pulling of type IV pili reveals their flexibility and adhesion to surfaces over extended lengths of the pili. Biophys J 2015;108:2865–75. https://doi.org/10.1016/j.bpj.2015.05.016.
[128] Mercier-Bonin M, Dehouche A, Morchain J, Schmitz P. Orientation and detachment dynamics of Bacillus spores from stainless steel under controlled shear flow: modelling of the adhesion force. Int J Food Microbiol 2011;146:182–91. https://doi.org/10.1016/j.ijfoodmicro.2011.02.025.
[129] Chen Y, Harapanahalli AK, Busscher HJ, Norde W, Van der Mei HC. Nanoscale cell wall deformation impacts long-range bacterial adhesion forces on surfaces. Appl Environ Microbiol 2014;80:637–43. https://doi.org/10.1128/AEM.02745-13.
[130] Busscher HJ, Van der Mei HC. How do bacteria know they are on a surface and regulate their response to an adhering state? PLoS Pathog 2012;8:e1002440. https://doi.org/10.1371/journal.ppat.1002440.
[131] Papenfort K, Bassler BL. Quorum sensing signal-response systems in Gram-negative bacteria. Nat Rev Microbiol 2016;14:576–88. https://doi.org/10.1038/nrmicro.2016.89.
[132] Gantner S, Schmid M, Durr C, Schuhegger R, Steidle A, Hutzler P, et al. *In situ* quantitation of the spatial scale of calling distances and population density-independent N-acylhomoserine lactone-mediated communication by rhizobacteria colonized on plant roots. FEMS Microbiol Ecol 2006;56:188–94. https://doi.org/10.1111/j.1574-6941.2005.00037.x.
[133] Darch SE, Simoska O, Fitzpatrick M, Barraza JP, Stevenson KJ, Bonnecaze RT, et al. Spatial determinants of quorum signaling in a *Pseudomonas aeruginosa* infection model. Proc Natl Acad Sci 2018;115:4779–84. https://doi.org/10.1073/pnas.1719317115.
[134] Gu J, Valdevit A, Chou T-M, Libera M. Substrate effects on cell-envelope deformation during early-stage*Staphylococcus aureus* biofilm formation. Soft Matter 2017;13:2967–76. https://doi.org/10.1039/c6sm02815b.
[135] Lee K, Hahn LD, Yuen WW, Vlamakis H, Kolter R, Mooney DJ. Metal-enhanced fluorescence to quantify bacterial adhesion. Adv Mater 2011;23:H101–4. https://doi.org/10.1002/adma.201004096.
[136] Malicka J, Gryczynski I, Gryczynski Z, Lakowicz JR. Effects of fluorophore-to-silver distance on the emission of cyanine-dye-labeled oligonucleotides. Anal Biochem 2003;315:57–66. https://doi.org/10.1016/S0003-2697(02)00702-9.
[137] Carniello V, Peterson BW, Sjollema J, Busscher HJ, Van der Mei HC. Surface enhanced fluorescence and nanoscopic cell wall deformation in adhering *Staphylococcus aureus* upon exposure to cell wall active and non-active antibiotics. Nanoscale 2018;10:11123–33. https://doi.org/10.1039/C8NR01669K.
[138] Iriya R, Syal K, Jing W, Mo M, Yu H, Haydel SE, et al. Real-time detection of antibiotic activity by measuring nanometer-scale bacterial deformation. J Biomed Opt 2017;22:1–9. https://doi.org/10.1117/1.JBO.22.12.126002.
[139] Dover RS, Bitler A, Shimoni E, Trieu-Cuot P, Shai Y. Multiparametric AFM reveals turgor-responsive net-like peptidoglycan architecture in live streptococci. Nat Commun 2015;6:7193. https://doi.org/10.1038/ncomms8193.
[140] Ellison CK, Kan J, Dillard RS, Kysela DT, Ducret A, Berne C, et al. Obstruction of pilus retraction stimulates bacterial surface sensing. Science 2017;358:535–8. https://doi.org/10.1126/science.aan5706 (80-).
[141] Crouzet M, Claverol S, Lomenech A-M, Le Sénéchal C, Costaglioli P, Barthe C, et al. *Pseudomonas aeruginosa* cells attached to a surface display a typical proteome early as 20 minutes of incubation. PLoS One 2017;12:e0180341. https://doi.org/10.1371/journal.pone.0180341.
[142] Rodesney CA, Roman B, Dhamani N, Cooley BJ, Katira P, Touhami A, et al. Mechanosensing of shear by *Pseudomonas aeruginosa* leads to increased levels of the cyclic-di-GMP signal initiating biofilm development. Proc Natl Acad Sci 2017;114:5906–11. https://doi.org/10.1073/pnas.1703255114.
[143] Harapanahalli AK, Chen Y, Li J, Busscher HJ, Van der Mei HC. Influence of adhesion force on *icaA* and *cidA* gene expression and production of matrix components in *Staphylococcus aureus* biofilms. Appl Environ Microbiol 2015;81:3369–78. https://doi.org/10.1128/AEM.04178-14.
[144] Cuthbertson L, Mainprize IL, Naismith JH, Whitfield C. Pivotal roles of the outer membrane polysaccharide export and polysaccharide copolymerase protein families in export of extracellular polysaccharides in Gram-negative bacteria. Microbiol Mol Biol Rev 2009;73:155–77. https://doi.org/10.1128/MMBR.00024-08.
[145] Morona R, Purins L, Tocilj A, Matte A, Cygler M. Sequence-structure relationships in polysaccharide co-polymerase (PCP) proteins. Trends Biochem Sci 2009;34:78–84. https://doi.org/10.1016/j.tibs.2008.11.001.
[146] Spoering AL, Gilmore MS. Quorum sensing and DNA release in bacterial biofilms. Curr Opin Microbiol 2006;9:133–7. https://doi.org/10.1016/j.mib.2006.02.004.
[147] Kester JC, Fortune SM. Persisters and beyond: mechanisms of phenotypic drug resistance and drug tolerance in bacteria. Crit Rev Biochem Mol Biol 2014;49:91–101. https://doi.org/10.3109/10409238.2013.869543.
[148] Carniello V, Harapanahalli AK, Busscher HJ, Van der Mei HC. Adhesion force sensing and activation of a membrane-bound sensor to activate nisin efflux pumps in *Staphylococcus aureus* under mechanical and chemical stresses. J Colloid Interface Sci 2018;512:14–20. https://doi.org/10.1016/j.jcis.2017.10.024.
[149] Iscla I, Blount P. Sensing and responding to membrane tension: the bacterial MscL channel as a model system. Biophys J 2012;103:169–74. https://doi.org/10.1016/j.bpj.2012.06.021.
[150] Perozo E, Kloda A, Cortes DM, Martinac B. Physical principles underlying the transduction of bilayer deformation forces during mechanosensitive channel gating. Nat Struct Biol 2002;9:696–703. https://doi.org/10.1038/nsb827.
[151] Najem JS, Dunlap MD, Rowe ID, Freeman EC, Grant JW, Sukharev S, et al. Activation of bacterial channel MscL in mechanically stimulated droplet interface bilayers. Sci Rep 2015;5:13726. https://doi.org/10.1038/srep13726.
[152] Janmey PA, Kinnunen PKJ. Biophysical properties of lipids and dynamic membranes. Trends Cell Biol 2006;16:538–46. https://doi.org/10.1016/j.tcb.2006.08.009.
[153] Levina N, Tötemeyer S, Stokes NR, Louis P, Jones MA, Booth IR, et al. Protection of *Escherichia coli* cells against extreme turgor by activation of MscS and MscL mechanosensitive channels: identification of genes required for MscS activity. EMBO J 1999;18:1730–7.
[154] Buda R, Liu Y, Yang J, Hegde S, Stevenson K, Bai F, et al. Dynamics of *Escherichia coli*'s passive response to a sudden decrease in external osmolarity. Proc Natl Acad Sci 2016;113:E5838–46. https://doi.org/10.1073/pnas.1522185113.
[155] Kocer A. Mechanisms of mechanosensing — mechanosensitive channels, function and re-engineering. Curr Opin Chem Biol 2015;29:120–7. https://doi.org/10.1016/j.cbpa.2015.10.006.
[156] Harapanahalli AK, Younes JA, Allan E, Van der Mei HC, Busscher HJ. Chemical signals and mechanosensing in bacterial responses to their environment. PLoS Pathog 2015;11:e1005057. https://doi.org/10.1371/journal.ppat.1005057.
[157] Rice KC, Mann EE, Endres JL, Weiss EC, Cassat JE, Smeltzer MS, et al. The *cidA* murein hydrolase regulator contributes to DNA release and biofilm development in *Staphylococcus aureus*. Proc Natl Acad Sci 2007;104:8118–33.
[158] Ranjit DK, Endres JL, Bayles KW. *Staphylococcus aureus* CidA and LrgA proteins exhibit holin-like properties. J Bacteriol 2011;193:2468–76. https://doi.org/10.1128/JB.01545-10.